

Scuola di Scienze
Dipartimento di Fisica e Astronomia
Corso di Laurea in Fisica

Analytical and numerical study of polarons

Relatore:

Prof. Cesare Franchini

Presentata da:

Nicolò Montalti

Correlatore:

Lorenzo Varrassi

Anno Accademico 2021/2022

Abstract

The aim of this thesis is to introduce the polaron concept and to perform a DFT numerical calculation of a small polaron in the rutile phase of TiO_2 . In the first chapters, we present an analytical study of small and large polarons, based on the Holstein and Fröhlich Hamiltonians. The necessary mathematical formalism and physics fundamentals are briefly reviewed in the first chapter. In the second part of the thesis, Density Functional Theory (DFT) is introduced together with the DFT+U correction and its implementation in the Vienna Ab-Initio Simulation Package (VASP). The calculation of a small polaron in rutile is then described and discussed at a qualitative level. The polaronic solution is compared with the one of a delocalized electron.

The calculation showed how the polaron creates a new energy level 0.70 eV below the conduction band. The energy level is visible both in the band structure diagram and in the density of states diagram. The electron is localized on a titanium atom, distorting the surrounding lattice. In particular, the four oxygen atoms closer to the titanium atom are displaced by 0.085 Å outwards, whereas the two further oxygen atoms by 0.023 Å. The results are compatible, at a qualitative level, with the literature. Further developments of this work may try to improve the precision of the results and to quantitatively compare them with the literature.

Sommario

Questa tesi si propone di introdurre il concetto di polarone e di presentare un calcolo DFT di uno small polaron nella fase rutilo del TiO_2 . Nei primi capitoli si analizzano gli small e large polarons da un punto di vista analitico, basato sulle Hamiltoniane di Holstein e di Fröhlich. Il formalismo matematico e le basi fisiche necessarie vengono introdotte nel primo capitolo. Nella seconda parte della tesi, si introducono la Density Functional Theory (DFT), una sua correzione (DFT+U), e la sua implementazione nel Vienna Ab-Initio Simulation Package (VASP). Un calcolo numerico di uno small polaron è poi descritto e discusso a livello qualitativo. La soluzione polaronica è confrontata con un quella di un elettrone delocalizzato nel materiale.

Il calcolo ha evidenziato come il polaron crei un nuovo stato energetico 0.70 eV sotto la banda di conduzione. Il nuovo livello energetico è visibile sia nella struttura a bande, sia nel grafico della densità degli stati. L'elettrone si localizza su un atomo di titanio, distorcendo il reticolo circostante. In particolare, i quattro atomi di ossigeno più vicini al titanio si allontano di 0.085 Å, mentre i due atomi più distanti di 0.023 Å. I risultati sono qualitativamente compatibili con la letteratura. Futuri sviluppi del lavoro possono cercare di migliorare la precisione del calcolo, per poi proporre un confronto quantitativo.

INDICE

Acknowledgements	vi
Introduction	vii
1 Review of fundamentals	1
1.1 Second quantization	1
1.1.1 Occupation number representation	1
1.1.2 Creation and annihilation operators	3
1.1.3 Commutation relations	5
1.1.4 Dynamical variables	6
1.2 Electrons and phonons in crystals	7
1.2.1 Crystal lattice	7
1.2.2 Electrons in crystals	8
1.2.3 Tight binding model	10
1.2.4 Phonons	12
1.2.5 Electron-phonon interaction	14
2 The polaron problem	18
2.1 Landau-Pekar model	18
2.2 Fröhlich polarons	20
2.2.1 Derivation of the Fröhlich Hamiltonian	20
2.2.2 Weak coupling limit	24
2.2.3 Strong coupling limit	27
2.3 Holstein polarons	28
2.3.1 Derivation of the Holstein Hamiltonian	29
2.3.2 Weak coupling limit	31
2.4 Small and large polarons	33
3 Density Functional Theory	35
3.1 Introduction to DFT	35
3.1.1 Ground state and density functional formalism	35
3.1.2 The Kohn-Sham Equations	37
3.1.3 DFT corrections: DFT+U	40
3.2 Implementation	41
3.3 Vienna Ab-initio Simulation Package	43
4 Simulation of a small polaron in rutile	45
4.1 Procedure	45
4.1.1 DFT and DFT+U calculation on rutile	45
4.1.2 Electron localization	47
4.1.3 Polaron	49
4.2 Results and discussion	49

4.2.1	DFT and DFT+U calculation on rutile	49
4.2.2	Electron localization	52
4.2.3	Polaron	52
5	Conclusions	55

ACKNOWLEDGEMENTS

This work would have not been possible without the help and the support of many people, more than this page could contain. Not only the ones who have contributed directly to it in the past months, but everyone I have met along the path of taking this degree.

First of all, I want to thank my supervisor Prof. Cesare Franchini for giving me the opportunity of working on such an interesting topic. I am grateful for the time he dedicated to me and to this work. I also want to thank Lorenzo Varrassi for the help he gave me in understanding how DFT and VASP work. I would not have been able to conclude this work without his advices. Finally, I am grateful to the Department of Physics of the University of Bologna for letting me use their HPC Cluster for running the calculations.

I want to thank my family, especially my parents and grandparents, for believing in me and encouraging my passion in Physics. This work is dedicated to my mother, who could not fulfill the dream of studying this subject like me. I thank my father for his patience, his support and for feeding my curiosity since I was child. I am grateful to my sisters, for bearing me talking about my work, and to my grandparents, for their support and their interest in my studies.

Between my friends, a special thanks goes to Mattia, Adriano, Alessandro and Pietro, for making me feel home in a city that has never been really mine. I will never be able to repay them for their heart-warming hospitality. I have to thank Alessandro in particular for all the time he dedicated to listening to me in the past years. I am also grateful to Claudia and Lorenzo for their friendship and all the time we spent together.

I also want to thank Lorenzo and Alice, who have been two invaluable peers in the path to obtaining this degree. In the past years, they played a major role in keeping my curiosity and my enthusiasm always high. They have been among the few people I could actually discuss my work with, and help me when I needed it.

A final, heartfelt, thanks goes to Edoardo, Thomas, Jakob F., Jakob S., Samira, Riley, and all the other wonderful people I met in Groningen. With them, I spent the best months of my studies. Each of them changed me in their own way, helping me discover a whole new me, and contributing making this experience unforgettable.

I hope that all these people will be as proud of this work as I am, even the ones who might not understand it.

INTRODUCTION

Lev Landau was the first to propose the concept of an auto-localized electron in a crystal in a 1933 paper [1]. The idea was then developed by Pekar in 1946, who considered a single electron interacting with a dielectric continuum medium [2, 3]. He was the first to use the term *polaron* to define an electron that localizes itself in a potential well self-generated by the polarization of the material. This interaction was shown to cause an enhancement of the effective mass and a localization of the wavefunction [4]. In their work, Landau and Pekar used a quantum mechanical description of the electron and a classical description of the medium. A full quantum mechanical description was then developed by Fröhlich [5] and Holstein [6], who formalized the distinction between large and small polarons.

Fröhlich considered an electron in a continuum, polarizable medium. In his model, the electron is assumed to interact only with longitudinal optical phonons. The interaction gives rise to the polarization of the material, which generates a potential well in which the electron localizes. Since the medium is treated as a continuum, the results are only valid for large polarons, that are polarons with an effective radius larger than the lattice constant. On the other hand, Holstein considered short-range electron-phonon interactions, resulting from the coupling between a carrier and the strain where it resides. Holstein theory takes into account the discreteness of the lattice, and it is used to describe small polarons, for which the effective radius is smaller than the lattice constant.

All the attempts to find analytical solutions to the Fröhlich Hamiltonian have been fruitless, whereas the Holstein Hamiltonian is exactly solvable only in the two-site case [7]. Approximation techniques and numerical simulations are then unavoidable. Good results in solving both the Fröhlich and Holstein Hamiltonians have been achieved with the Diagrammatic Quantum Monte Carlo method [8, 9]. For small polarons, DFT+U methods have also proven to be applicable [10]. A rigorous, ab initio computational theory of polarons was recently developed by Feliciano Giustino and colleagues combining the Landau–Pekar model with DFT [11].

OUTLINE

The aim of this thesis is to give an introductory analytical description of polarons and to perform a numerical simulation of a small polaron in rutile. The focus of the analytical discussion is to derive Holstein and Fröhlich Hamiltonians. The numerical calculation aims to simulate a small polaron in rutile TiO_2 .

In Chapter 1, we introduce the mathematical formalism and physical laws necessary

for the study of polarons. We start by reviewing the second quantization formalism, and use it to describe electrons and phonons in crystals. Electrons and phonons are firstly studied as non-interacting particles. Then, the electron-phonon interaction, essential for the description of polarons, is investigated as well.

In Chapter 2, the theory of polarons is explained starting by the original Landau-Pekar model. Then, Fröhlich and Holstein Hamiltonians are derived and solved in the small and large coupling regimes. Lastly, small and large polarons main properties are discussed and compared.

In Chapter 3, Density Functional Theory (DFT) is presented. The theory behind it is explained together with some of its problems. An extension of it, DFT+U, is also introduced to solve some inaccuracies. Lastly, its implementation is discussed focusing on the Vienna Ab-initio Simulation Package (VASP).

In Chapter 4, we present a simulation of a small polaron in TiO_2 . The whole simulation process is described, and the results are discussed. The polaronic solution is compared with an electron delocalized in the material, with particular emphasis on the density of states, band structure and charge isosurfaces.

REVIEW OF CONDENSED MATTER PHYSICS FUNDAMENTALS

Before discussing polarons and their properties, we offer a brief review of some fundamentals of condensed matter physics. We start by discussing the second quantization formalism, which will be used extensively in the rest of the thesis. Then, we briefly describe the behaviour of electrons and phonons in materials. Electrons and phonons are initially studied as non-interacting. Then, their interaction, which serves as a basis for the description of polarons, is discussed as well.

1.1 SECOND QUANTIZATION

Second quantization, also referred to as occupation number representation, is a formalism used to describe and analyse quantum many-body systems. The key ideas of this method were introduced in 1927 by Paul Dirac [12], and were later developed by Vladimir Fock and Pascual Jordan [13]. The key idea of second quantization is to represent states of a many-body system as elements of a Fock space. The elements of a Fock space are labelled by the number of particles in each single-particle state. The individual single-particle states are neglected, focusing only on the whole system.

1.1.1 Occupation number representation

In condensed matter physics we often have to deal with systems of many particles. We can describe such a system starting from the wavefunctions of the single particles $|k\rangle$, where the particle is in an eigenstate of eigenvalue k of the operator \hat{K} . We suppose this set of vectors to be orthonormal. A first approach to describe the system could be to write the total state vector as the product of the single-particle states.

$$|\Psi\rangle = |k_1\rangle |k_2\rangle \dots |k_N\rangle \quad (1.1)$$

However, the former expression does not take into account the indistinguishability of quantum particles. In fact, the physics of the system must be invariant under the exchange of two particles. This is possible only if $|\Psi\rangle$ is either symmetric or antisymmetric for the exchange of two particles. The former case is true for bosons, the latter for fermions.

In order to satisfy this condition, we have to modify Eq. (1.1). An appropriate

linear combination of the products of the single kets, compatible with the symmetry constraints required by Bose and Fermi statistics is given by

$$|\Psi\rangle = |k_1, k_2, \dots, k_N\rangle = \sqrt{\frac{1}{N!}} \sum_P \xi^P |P[k_1]\rangle |P[k_2]\rangle \dots |P[k_N]\rangle \quad (1.2)$$

where the sum is taken over the $N!$ permutations P of k_1, k_2, \dots, k_N . The constant ξ is equal to 1 for bosons and -1 for fermions. For fermions, $\xi^P = 1$ for even permutations and $\xi^P = -1$ for odd permutations. This construction assures that the total wavefunction is symmetric for the exchange of two bosons and antisymmetric for the exchange of two fermions. It is important to notice that Eq. (1.2) has an ambiguity in the phase of the final vector. To remove it, we chose the permutation to be even when $k_1 < k_2 < \dots < k_N$.

It is useful to compute the product of a basis bra and a basis ket of two total state vectors.

$$\begin{aligned} \langle m_1, \dots, m_N | k_1, \dots, k_N \rangle &= \frac{1}{N!} \\ &= \sum_P \sum_{P'} \xi^{P+P'} \langle P[m_1] | \langle P[m_2] | \dots \langle P[m_N] | \times |P'[k_1]\rangle |P'[k_2]\rangle \dots |P'[k_N]\rangle \\ &= \sum_{P''} \xi^{P''} \langle m_1 | P''[k_1]\rangle \dots \langle m_N | P''[k_N]\rangle \\ &= \left| \begin{array}{cccc} \langle m_1 | k_1 \rangle & \langle m_1 | k_2 \rangle & \dots & \langle m_1 | k_N \rangle \\ \langle m_2 | k_2 \rangle & \langle m_2 | k_3 \rangle & \dots & \langle m_2 | k_N \rangle \\ \dots & \dots & \dots & \dots \\ \langle m_N | k_1 \rangle & \langle m_N | k_2 \rangle & \dots & \langle m_N | k_N \rangle \end{array} \right|_\xi \quad (1.3) \end{aligned}$$

where $|\cdot|_{\xi=-1}$ represents a determinant and $|\cdot|_{\xi=1}$ a permanent (a determinant with all positive signs). Given the orthonormality of the single state kets, the only terms of the sum that differ from zero are the ones where

$$P''\{k_1, \dots, k_N\} = \{m_1, \dots, m_N\} \quad (1.4)$$

If a state is composed of n_j bosons in the state k_j , the norm squared of the state vector is equal to the total number of identical permutations

$$\langle k_1, \dots, k_N | k_1, \dots, k_N \rangle = n_1! n_2! \dots n_N! \quad (1.5)$$

Thus, the normalized state vector is

$$|k_1, \dots, k_N\rangle_n = \frac{1}{\sqrt{n_1! n_2! \dots n_N!}} |k_1, \dots, k_N\rangle \quad (1.6)$$

The case of fermions is easier. Since n_j can only be either 1 or 0, there is only one identical permutation and the state is already normalized.

Given the indistinguishability of the particles, a simpler way to describe this state vector is using only the number n_j of particles that are in the state k_j .

$$|n_1, n_2, \dots, n_i, \dots\rangle = |k_1, \dots, k_N\rangle_n \quad (1.7)$$

where k_j is repeated n_j times. This eliminates the inconvenience of having multiple kets describing the same state as we had before. This representation is called occupation number representation, and the kets are said to be elements of the Fock space.

Two special cases of states in the Fock space are the following. The vacuum state

$$|0, 0, \dots, 0\rangle = |\emptyset\rangle \quad (1.8)$$

is a state with no particles in any single-particle states, and

$$|0, 0, \dots, n_i = 1, \dots\rangle = |k_i\rangle \quad (1.9)$$

is a state with exactly one particle in the k_i state.

1.1.2 Creation and annihilation operators

Now that we have defined the basis kets, we can introduce two operators that are used to transform them. We define the *creation operator* as

$$\hat{a}_i^\dagger |k_1, k_2, \dots\rangle = |k_i, k_1, k_2, \dots\rangle \quad (1.10)$$

and the *annihilation operator* \hat{a}_i as its adjoint. Below, we show several properties that derive from this definition, but its essential role can be understood by applying it to the vacuum state.

$$\hat{a}_i^\dagger |\emptyset\rangle = |k_i\rangle \quad (1.11)$$

Its effect is to add a particle in the state k_i to the system. It is also easy to interpret the role of the *annihilation operator*, in fact

$$1 = \langle k_i | k_i \rangle = \langle \emptyset | \hat{a}_i \hat{a}_i^\dagger | \emptyset \rangle = \langle \emptyset | \hat{a}_i | k_i \rangle \quad (1.12)$$

which implies that

$$\hat{a}_i |k_i\rangle = |\emptyset\rangle \quad (1.13)$$

We now try to prove these properties on a general basis ket. We consider the transition matrix element

$$\begin{aligned} \mathcal{A} &= \langle m_1, \dots, m_{N-1} | \hat{a}_i | k_1, \dots, k_N \rangle = \\ &= \langle k_1, \dots, k_N | \hat{a}_i^\dagger | m_1, \dots, m_{N-1} \rangle^* = \langle k_1, \dots, k_N | k_i, m_1, \dots, m_{N-1} \rangle^* \end{aligned} \quad (1.14)$$

and, using Eq. (1.3), we write it as the determinant

$$\mathcal{A} = \begin{vmatrix} \langle k_1 | k_i \rangle & \langle k_1 | m_1 \rangle & \dots & \langle k_1 | m_{N-1} \rangle \\ \langle k_2 | k_i \rangle & \langle k_2 | m_1 \rangle & \dots & \langle k_2 | m_{N-1} \rangle \\ \dots & \dots & \dots & \dots \\ \langle k_N | k_i \rangle & \langle k_N | m_1 \rangle & \dots & \langle k_N | m_{N-1} \rangle \end{vmatrix}_{\xi}^* \quad (1.15)$$

Developing it along the first column, we find

$$\begin{aligned} \mathcal{A} &= \left(\sum_{j=1}^N \xi^{j+1} \langle k_j | k_i \rangle \begin{vmatrix} \langle k_1 | m_1 \rangle & \dots & \langle k_1 | m_{N-1} \rangle \\ \langle k_2 | m_1 \rangle & \dots & \langle k_2 | m_{N-1} \rangle \\ \dots & (no k_j) & \dots \\ \langle k_N | m_1 \rangle & \dots & \langle k_N | m_{N-1} \rangle \end{vmatrix}_{\xi} \right)^* \\ &= \sum_{j=1}^N \xi^{j+1} \langle k_i | k_j \rangle \langle k_1, \dots, (no k_j), k_N | m_1, \dots, m_{N-1} \rangle^* \\ &= \sum_{j=1}^N \xi^{j+1} \delta_{k_i k_j} \langle m_1, \dots, m_{N-1} | k_1, \dots, (no k_j), k_N \rangle \quad (1.16) \end{aligned}$$

and confronting Eq. (1.16) with Eq. (1.14) we conclude

$$\begin{aligned} \hat{a}_i |k_1, \dots, k_N\rangle &= \sum_{j=1}^N \xi^{j+1} \langle k_i | k_j \rangle |k_1, \dots, (no k_j), k_N\rangle \\ &= \sum_{j=1}^N \xi^{j+1} \delta_{k_i k_j} |k_1, \dots, (no k_j), k_N\rangle \quad (1.17) \end{aligned}$$

If k_i is not present in $|k_1, \dots, k_N\rangle$, $\delta_{k_i k_j} = 0$ and overall $\hat{a}_i |k_1, \dots, k_N\rangle = 0$. On the other hand, if k_i is included in the ket n_i times, there are n_i non-null terms in the sum. Thus, in the case of bosons,

$$\hat{a}_i |k_1, \dots, k_N\rangle = n_i |k_1, \dots, (one less k_i), k_N\rangle \quad (1.18)$$

We can use Eq. (1.7) to express the last relation in the occupation number representation.

$$\begin{aligned} \hat{a}_i |n_1, n_2, \dots, n_i, \dots\rangle &= \hat{a}_i |k_1, \dots, k_N\rangle_n \\ &= \hat{a}_i \left(\prod_{j=1}^N \sqrt{n_j!} \right)^{-1} |k_1, \dots, k_N\rangle = n_i \left(\prod_{j=1}^N \sqrt{n_j!} \right)^{-1} |k_1, \dots, (one less k_i), k_N\rangle \\ &= \sqrt{n_i} |k_1, \dots, (one less k_i), k_N\rangle_n = \sqrt{n_i} |n_1, n_2, \dots, n_i - 1, \dots\rangle \quad (1.19) \end{aligned}$$

The same argument, developed for the creation operator \hat{a}_i^\dagger , leads to

$$\hat{a}_i^\dagger |n_1, n_2, \dots, n_i, \dots\rangle = \sqrt{n_i + 1} |n_1, n_2, \dots, n_i + 1, \dots\rangle \quad (1.20)$$

For fermions, the occupation numbers can either be 1 or 0. The creation operator \hat{a}_i^\dagger returns zero if $n_i = 1$ and a phase factor of ± 1 if $n_i = 0$. The annihilation operator \hat{a}_i does the opposite.

We can define another useful operator, the number operator $\hat{N}_i = \hat{a}_i^\dagger \hat{a}_i$. If we apply it to a basis ket, we find

$$\begin{aligned}\hat{N}_i |n_1, n_2, \dots, n_i, \dots\rangle &= \hat{a}_i^\dagger \hat{a}_i |n_1, n_2, \dots, n_i, \dots\rangle \\ &= \hat{a}_i^\dagger \sqrt{n_i} |n_1, n_2, \dots, n_i - 1, \dots\rangle = n_i |n_1, n_2, \dots, n_i, \dots\rangle\end{aligned}\quad (1.21)$$

From Eq. (1.21), it is clear that the number operator \hat{N}_i , as the name suggests, returns the number of bosons in the state k_i in the system.

1.1.3 Commutation relations

All the properties of the creation and annihilation operators can be deduced from their (anti)commutation relations, which will be derived in this section. Applying $\hat{a}_{k'}^\dagger \hat{a}_k^\dagger$ on a basis ket, and using Eq. (1.10), we find

$$\begin{aligned}\hat{a}_{k'}^\dagger \hat{a}_k^\dagger |k_1, k_2, \dots\rangle &= |k', k, k_1, k_2, \dots\rangle \\ &= \xi |k, k', k_1, k_2, \dots\rangle = \xi \hat{a}_k^\dagger \hat{a}_{k'}^\dagger |k_1, k_2, \dots\rangle\end{aligned}\quad (1.22)$$

which implies the (anti)commutation relation

$$\hat{a}_k^\dagger \hat{a}_{k'}^\dagger - \xi \hat{a}_{k'}^\dagger \hat{a}_k^\dagger = [\hat{a}_k^\dagger, \hat{a}_{k'}^\dagger]_\xi = 0 \quad (1.23)$$

where $[A, B]_{-1} = \{A, B\} = AB + BA$ and $[A, B]_1 = AB - BA$. We see that for bosons the creation operators always commute, while for fermions they anti-commute.

Let's now investigate the commutator of a creation and an annihilation operator. Using Eq. (1.10) and Eq. (1.17)

$$\begin{aligned}\hat{a}_{k'} \hat{a}_k^\dagger |k_1, k_2, \dots\rangle &= \hat{a}_{k'} |k, k_1, k_2, \dots\rangle \\ &= \langle k' | k \rangle |k_1, k_2, \dots\rangle + \sum_j \xi^j \langle k' | k_j \rangle |k, k_1, k_2, (\text{no } k_j) \dots\rangle\end{aligned}\quad (1.24)$$

$$\begin{aligned}\hat{a}_k^\dagger \hat{a}_{k'} |k_1, k_2, \dots\rangle &= \hat{a}_k^\dagger \sum_j \xi^{j+1} \langle k' | k_j \rangle |k_1, k_2, (\text{no } k_j) \dots\rangle \\ &= \sum_j \xi^{j+1} \langle k' | k_j \rangle |k, k_1, k_2, (\text{no } k_j) \dots\rangle\end{aligned}\quad (1.25)$$

thus

$$(\hat{a}_{k'} \hat{a}_k^\dagger - \xi \hat{a}_k^\dagger \hat{a}_{k'}) = \langle k' | k \rangle |k_1, k_2, \dots\rangle \quad (1.26)$$

and

$$[\hat{a}_{k'}, \hat{a}_k^\dagger]_\xi = \langle k' | k \rangle = \delta_{kk'} \quad (1.27)$$

The previous equation is of fundamental importance in second quantization formalism. If we have a set of single-state basis kets $|k\rangle$, and we define a creation and annihilation operator that satisfy Eq. (1.27), we obtain multi-particle basis kets $|k_1, k_2, \dots\rangle$ that automatically satisfy the symmetry condition of Fermi and Bose statistics. The kets can then be expressed in the more compact occupation number representation $|n_1, n_2, \dots\rangle$.

1.1.4 Dynamical variables

The final aim of second-quantization is to express every operator in terms of the creation and annihilation operators. The action of every operator can be interpreted as a combination of the creation (\hat{a}^\dagger), annihilation (\hat{a}) and counting (\hat{N}) of the particles in the system. This allows us to use Fock states as kets and to simplify our equations. We focus our discussion on additive single-particle operator. Examples are momentum, kinetic energy and single body potentials. In these cases, the total expectation value of the operator is simply given by the sum of the expectation values of the operator applied to the single particles [14].

Given an operator \hat{K} of eigenkets $|k_i\rangle$, with $\hat{K}|k_i\rangle = k_i|k_i\rangle$, and a state vector

$$|\Psi\rangle = |n_1, n_2, \dots\rangle \quad (1.28)$$

the result of applying \hat{K} to $|\Psi\rangle$ is simply

$$\hat{K}|\Psi\rangle = \left(\sum_i n_i k_i \right) |\Psi\rangle \quad (1.29)$$

Confronting this expression with the definition of the number operator expressed in Eq. (1.21) we can write \hat{K} as

$$\hat{K} = \sum_i k_i \hat{N}_i = \sum_i k_i \hat{a}_i^\dagger \hat{a}_i \quad (1.30)$$

It could happen to have a state ket expressed in a basis different from the eigenkets of our operator of interest. If we suppose this basis to be formed by $|l_j\rangle$, using the relation of completeness,

$$|k_i\rangle = \sum_j |l_j\rangle \langle l_j | k_i \rangle \quad (1.31)$$

It makes then sense to write

$$\hat{a}_i^\dagger = \sum_j \hat{b}_j^\dagger \langle l_j | k_i \rangle \quad (1.32)$$

which implies

$$\hat{a}_i = \sum_j \hat{b}_j \langle k_i | l_j \rangle \quad (1.33)$$

where operators \hat{b}_j^\dagger and \hat{b}_j create and annihilate the single-particle states $|l_j\rangle$. The result of applying Eq. (1.32) on the vacuum state is then

$$\hat{a}_i^\dagger |0\rangle = \sum_j \hat{b}_j^\dagger \langle l_j | k_i \rangle |0\rangle = \sum_j |l_j\rangle \langle l_j | k_i \rangle = |k_i\rangle \quad (1.34)$$

in agreement with Eq. (1.31).

We are now ready to express the operator \hat{K} in the basis $|l_j\rangle$.

$$\begin{aligned} \hat{K} &= \sum_i k_i \hat{a}_i^\dagger \hat{a}_i = \sum_i k_i \sum_{mn} \hat{b}_m^\dagger \hat{b}_n \langle l_m | k_i \rangle \langle k_i | l_n \rangle \\ &= \sum_{mn} \hat{b}_m^\dagger \hat{b}_n \sum_i \langle l_m | k_i \rangle k_i \langle k_i | l_n \rangle = \sum_{mn} \hat{b}_m^\dagger \hat{b}_n \langle l_m | \left[\hat{K} \sum_i |k_i\rangle \langle k_i| \right] |l_n\rangle \\ &= \sum_{mn} \langle l_m | \hat{K} | l_n \rangle \hat{b}_m^\dagger \hat{b}_n \end{aligned} \quad (1.35)$$

This allows us to write every additive operator in terms of the creation and annihilation operators. For example, it is possible to write the Hamiltonian for a non-interacting system of particles, where the potential and the kinetic energy satisfy the additivity requirement, as

$$\hat{H} = \sum_{mn} \langle l_m | \hat{T} + \hat{V}_1 | l_n \rangle \hat{b}_m^\dagger \hat{b}_n \quad (1.36)$$

where V_1 is the non-interacting potential and \hat{T} the kinetic energy of the single particle.

1.2 ELECTRONS AND PHONONS IN CRYSTALS

In this section we briefly describe how free electrons and phonons behave in crystals, starting with a description of the crystal lattice. Initially, the electron-electron, phonon-phonon and electron-phonon interactions are not considered. Eventually, the electron-phonon interaction is discussed, as this represent the key interaction of the polaron quasiparticle.

1.2.1 Crystal lattice

Condensed matter physics has to deal with systems of many particles, typically electrons. We have already introduced a mathematical formalism that allows us to describe such systems. However, it is clearly impossible to solve the equations of a general

N-body system. Luckily, X-ray diffraction experiments showed that many solids exhibit particular symmetry properties, useful to simplify the problem.

Many solids, called crystals, are composed by the repetition in space of an identical unit cell. The unit cell is defined as the smallest repeating unit having the full symmetry of the crystal structure. The Bravais lattice, also referred to as space lattice, describes the geometric arrangement of the unit cells. The unit cells are positioned on the lattice points belonging to the Bravais lattice. Given two lattice points, positioned at \mathbf{R}_1 and \mathbf{R}_2 , the difference between them is

$$\mathbf{R}_1 - \mathbf{R}_2 = \mathbf{R}_n \quad (1.37)$$

where $\mathbf{R}_n = n_1 \mathbf{a}_1 + n_2 \mathbf{a}_2 + n_3 \mathbf{a}_3$. The three vectors $\mathbf{a}_1, \mathbf{a}_2, \mathbf{a}_3$ are called basis vectors and n_1, n_2, n_3 are integers. The position of a single atom in the crystal can then be expressed as the sum of its position in the unit cell τ_a and the position of the lattice point \mathbf{R}_n in the crystal

$$\mathbf{R}_n^a = \mathbf{R}_n + \tau_a \quad (1.38)$$

Given the symmetry of the system, every property $f(\mathbf{r})$ of the lattice is invariant under a translation of a lattice vector \mathbf{R}_n

$$f(\mathbf{r} + \mathbf{R}_n) = f(\mathbf{r}) \quad (1.39)$$

We will see that applying this simple principle to the potential generated by the ions will have important implications on the description of electrons.

Associated to the Bravais lattice, there is a second lattice called reciprocal lattice. It is defined by three other basis vectors $\mathbf{b}_1, \mathbf{b}_2, \mathbf{b}_3$, with

$$\mathbf{b}_1 = \frac{2\pi}{\Omega} \mathbf{a}_2 \times \mathbf{a}_3 \quad \mathbf{b}_2 = \frac{2\pi}{\Omega} \mathbf{a}_3 \times \mathbf{a}_1 \quad \mathbf{b}_3 = \frac{2\pi}{\Omega} \mathbf{a}_1 \times \mathbf{a}_2 \quad (1.40)$$

where $\Omega = |\mathbf{a}_1 \cdot \mathbf{a}_2 \times \mathbf{a}_3|$ is the volume of the unit cell. A vector in the reciprocal lattice is usually written as $\mathbf{G}_m = m_1 \mathbf{b}_1 + m_2 \mathbf{b}_2 + m_3 \mathbf{b}_3$, where m_1, m_2, m_3 are integers. From Eq. (1.40) it is easy to see that the product of a basis Bravais lattice vector \mathbf{a}_i and a basis reciprocal lattice vector \mathbf{b}_j is

$$\mathbf{a}_i \cdot \mathbf{b}_j = 2\pi \delta_{ij} \quad (1.41)$$

1.2.2 Electrons in crystals

The simplest quantum-mechanical model for electrons is the Sommerfeld model. It was developed by Arnold Sommerfeld in 1928 [15], combining the Drude model [16] with Fermi-Dirac statistics. The electrons are treated as quantum non-interacting free particles, which implies that the wavefunctions are plane waves

$$\psi_{\mathbf{k}} = e^{i\mathbf{k} \cdot \mathbf{r}} \quad (1.42)$$

The energy is entirely kinetic, and the dispersion relation is

$$\epsilon_{\mathbf{k}} = \frac{\hbar^2 k^2}{2m} \quad (1.43)$$

Despite its simplicity, this model is surprisingly good at describing a vast number of physical phenomena. Examples are the Wiedemann–Franz law, electrons heat capacity and electrical conductivity. However, it does not give any explanation for the different properties of conductors, insulators and semiconductors. To correctly describe the properties of electrons, we have to take into account the potential generated by the ions in the crystal. The interaction is entirely electrical, so the potential is the well-known Coulomb potential

$$V_{e-N} = \sum_{i=1}^{N_e} \sum_{j=1}^{N_N} \frac{1}{4\pi\epsilon_0} \frac{-Z_j e^2}{|\mathbf{r}_i - \mathbf{R}_j|} \quad (1.44)$$

where the first sum is taken over the electrons and the second over the nuclei. It is convenient to divide the electrons in inner core electrons and valence electrons. The formers are tightly bound to the nucleus and occupy closed inner shells. They do not interact with the other atoms of the crystal, so the nucleus together with its core electrons can be treated as a positive ion. The valence electrons, belonging to non-closed shells, form chemical bonds with other atoms. Despite this description of electrons being apparently simpler, the interaction between valence electrons and ions cannot be described by a simple Coulomb potential between the electrons and the nucleus V_{e-N} . The new potential V_{e-I} , used to describe the interaction between the valence electrons and the ion, has to take into account the core electrons as well.

The potential V_{e-I} has not a simple known form. To overcome the complexity of solving a many-body Schrödinger equation with a long range electromagnetic interaction, we exploit the symmetry of the crystal. Recalling our previous discussion, we know that the potential of the ions is translationally invariant:

$$V_{e-I}(\mathbf{r} + \mathbf{R}_n) = V_{e-I}(\mathbf{r}) \quad (1.45)$$

where \mathbf{r} is the position of the electron and \mathbf{R}_n is a Bravais lattice vector. The Schrödinger equation for the periodic potential V_{e-I} is then

$$\hat{H}_{\text{Bloch}} \Psi = \left(-\frac{\hbar^2}{2m} \nabla^2 + V_{e-I} \right) \Psi = \epsilon \Psi \quad (1.46)$$

Bloch proved in 1929 that this problem is solved by the so-called Bloch functions

$$\hat{H}_{\text{Bloch}} \Psi_{n\mathbf{k}} = \epsilon_n(\mathbf{k}) \Psi_{n\mathbf{k}} \rightarrow \Psi_{n\mathbf{k}}(\mathbf{r}) = u_{n\mathbf{k}}(\mathbf{r}) e^{i\mathbf{k}\cdot\mathbf{r}} \quad (1.47)$$

where $u(\mathbf{r})$ is a function with the same periodicity of V_{e-I} , \mathbf{k} is a wavevector and n is the band index [17]. The plane wave solution showed in Eq. (1.42) is a simple case of

Eq. (1.47), where $V_{e-I}(\mathbf{r}) = 0$ and $u(\mathbf{r}) = 1$. An important consequence of the Bloch theorem is that the solutions to the Schrödinger equation, even if they are not plane waves, can still be indexed with the quantum number \mathbf{k} , along with the band index n .

Expanding $\epsilon_n(\mathbf{k})$ around $\mathbf{k} = 0$, for an isotropic energy band,

$$\epsilon_n(\mathbf{k}) = \epsilon_n(0) + \frac{\hbar k^2}{2m^*} + \mathcal{O}(k^3) \quad (1.48)$$

where m^* is the effective mass, defined as

$$\frac{1}{m^*} = \frac{1}{\hbar^2} \frac{\partial^2 \epsilon}{\partial k^2} \quad (1.49)$$

Expression (1.48) is formally identical to Eq. (1.43) with m^* in place of m . For small values of k , electrons can then be treated as particles of mass m^* .

We can now define a creation and an annihilation operator $\hat{c}_{n\mathbf{k}}^\dagger, \hat{c}_{n\mathbf{k}}$ as operators that create and annihilate an electron in the state (\mathbf{k}, n) . Using Eqs. (1.30) and (1.47), the final non-interacting electron Hamiltonian can be rewritten in second quantization as

$$\hat{H}_{el} = \sum_{n\mathbf{k}} \epsilon_{n\mathbf{k}} \hat{c}_{n\mathbf{k}}^\dagger \hat{c}_{n\mathbf{k}} \quad (1.50)$$

1.2.3 Tight binding model

The simplest models that describe electrons taking into account the potential of the lattice are the *nearly-free electrons model* and the *tight-binding model*. These two models approach the problem from an almost opposite point of view. If in the *nearly-free electrons model* electrons are treated as free particles perturbed by the ionic potential, in the *tight-binding model* electrons are treated as tightly bounded to the atoms. We are interested in exploring the latter, since it is used to describe electrons in the Holstein Hamiltonian.

Since the electrons are tightly bounded to the atoms, we suppose their wavefunction to be a linear combination of the atomic orbitals. The atomic orbitals ϕ_{ta} are functions that satisfy the equation

$$\left(\frac{\mathbf{p}^2}{2m} + V_a(\mathbf{r}) \right) \phi_{ta} = E_{ta} \phi_{ta} \quad (1.51)$$

where V_a is the potential generated by an ion of type a and t labels the different atomic states. We form a linear combination of the atomic orbitals which will be used as a basis to expand the electron wavefunction

$$\phi_k^{ta}(\mathbf{r}) = \frac{1}{\sqrt{N}} \sum_n e^{i\mathbf{k} \cdot \mathbf{R}_n} \phi_{ta}(\mathbf{r} - \mathbf{R}_n - \boldsymbol{\tau}_a) \quad (1.52)$$

where N is the number of unit cells. The factor $e^{ik \cdot R_n}$ ensures that ψ is of the Bloch form.

In the tight-binding approximation, an electron wavefunction is expressed as a linear combination of the atomic orbitals in Eq. (1.52):

$$\psi_k(\mathbf{r}) = \sum_{ta} c_{ta}(k) \phi_k^{ta}(\mathbf{r}) \quad (1.53)$$

We could now solve the Schrödinger equation, but we follow a different approach that is useful for the description of Holstein polarons. We want to express and solve the tight-binding electron Hamiltonian in a second-quantized form.

We start by analysing a system of free electrons. Using Eq. (1.50), we can write the Hamiltonian as

$$\hat{H}_{\text{free}} = \sum_{\mathbf{k}} \epsilon_{\mathbf{k}} \hat{c}_{\mathbf{k}}^{\dagger} \hat{c}_{\mathbf{k}} \quad (1.54)$$

where the sum is taken over the extended Brillouin zone, and

$$\epsilon_{\mathbf{k}} = \frac{\hbar^2 k^2}{2m} \quad (1.55)$$

The creation and annihilation operators in the momentum space are related to the respective creation and annihilation operators in the position space by a Fourier transformation

$$\hat{c}_{\mathbf{k}}^{\dagger} = \frac{1}{\sqrt{N}} \sum_j e^{i\mathbf{k} \cdot \mathbf{R}_j} \hat{c}_j^{\dagger} \quad (1.56)$$

$$\hat{c}_{\mathbf{k}} = \frac{1}{\sqrt{N}} \sum_j e^{-i\mathbf{k} \cdot \mathbf{R}_j} \hat{c}_j \quad (1.57)$$

Using Eqs. (1.56) and (1.57) we can write the Hamiltonian in the position space as

$$\hat{H}_{\text{free}} = \frac{1}{N} \sum_{ij} \sum_{\mathbf{k}} \epsilon_{\mathbf{k}} e^{i\mathbf{k} \cdot (\mathbf{R}_i - \mathbf{R}_j)} \hat{c}_i^{\dagger} \hat{c}_j \quad (1.58)$$

where N is the number of available \mathbf{k} states. It is easy to interpret the effect of the creation and annihilation operators in Eq. (1.58): an electron moves from \mathbf{R}_j to \mathbf{R}_i and

$$\tilde{t}_{ij} = \sum_{\mathbf{k}} \epsilon_{\mathbf{k}} e^{i\mathbf{k} \cdot (\mathbf{R}_i - \mathbf{R}_j)} \quad (1.59)$$

is the associated energy.

If we consider a system of non-interacting electrons moving in a Bravais lattice, subject to a periodic ionic potential, the dispersion relation in Eq. (1.55) will change. Thus, the factor \tilde{t}_{ij} will change too. We will refer to the new factor t_{ij} as the *hopping parameter*. It can still be interpreted as the change in energy after an electron moves

from the site j to the site i . The result is that the electrons will tend to become more localized, since the value of t_{ij} will be very small for large distances $|\mathbf{R}_i - \mathbf{R}_j|$. In the tight-binding approximation, we assume

$$t_{ij} = \begin{cases} -t & \text{for nearest neighbors} \\ 0 & \text{otherwise} \end{cases} \quad (1.60)$$

The tight-binding Hamiltonian becomes

$$\hat{H}_{tb} = -t \sum_{\langle i,j \rangle} (\hat{c}_i^\dagger \hat{c}_j + \hat{c}_j^\dagger \hat{c}_i) \quad (1.61)$$

where $\langle i,j \rangle$ means that the sum is extended only over the (i,j) that are nearest neighbours.

It is useful to express Eq. (1.61) in the momentum-space representation. In order to do so, we rewrite Eq. (1.61) as

$$\hat{H}_{tb} = -t \sum_{\langle i,j \rangle} (\hat{c}_i^\dagger \hat{c}_j + \hat{c}_j^\dagger \hat{c}_i) = -\frac{t}{2} \sum_i \sum_\delta (\hat{c}_i^\dagger \hat{c}_{i+\delta} + \hat{c}_{i+\delta}^\dagger \hat{c}_i) \quad (1.62)$$

where the sum over δ is taken over all the nearest neighbours of the site i and the factor $1/2$ is inserted to avoid double counting. Using Eqs. (1.56) and (1.57), we can express the Hamiltonian in the momentum-space representation:

$$\begin{aligned} \hat{H}_{tb} &= -\frac{t}{2} \frac{1}{N} \sum_i \sum_\delta \sum_{\mathbf{k}, \mathbf{k}'} (e^{-i\mathbf{k} \cdot \mathbf{R}_i} e^{i\mathbf{k}' \cdot (\mathbf{R}_i + \mathbf{R}_\delta)} \hat{c}_\mathbf{k}^\dagger \hat{c}_{\mathbf{k}'} + e^{i\mathbf{k} \cdot \mathbf{R}_i} e^{-i\mathbf{k}' \cdot (\mathbf{R}_i + \mathbf{R}_\delta)} \hat{c}_\mathbf{k}^\dagger \hat{c}_{\mathbf{k}'}) \\ &= -\frac{t}{2} \sum_{\mathbf{k}, \delta} (e^{i\mathbf{k} \cdot \mathbf{R}_\delta} + e^{-i\mathbf{k} \cdot \mathbf{R}_\delta}) \hat{c}_\mathbf{k}^\dagger \hat{c}_\mathbf{k} = -t \sum_{\mathbf{k}, \delta} \cos(\mathbf{k} \cdot \mathbf{R}_\delta) \hat{c}_\mathbf{k}^\dagger \hat{c}_\mathbf{k} \end{aligned} \quad (1.63)$$

which can be written as

$$\hat{H}_{tb} = \sum_{\mathbf{k}} \epsilon_{\mathbf{k}}^{tb} \hat{c}_\mathbf{k}^\dagger \hat{c}_\mathbf{k} \quad (1.64)$$

with

$$\epsilon_{\mathbf{k}}^{tb} = -t \sum_{\delta} \cos(\mathbf{k} \cdot \mathbf{R}_\delta) \quad (1.65)$$

1.2.4 Phonons

So far, we have treated the crystal as a collection of electrons subject to the potential of the ions fixed in the lattice. However, the ions are not really fixed. The crystal is held together by the bonds between the atoms. If we write the potential of the bonding force between two ions i and j as $v_{I-I}(|\mathbf{R}_i - \mathbf{R}_j|)$, the total ionic potential is

$$V_{I-I}(\mathbf{R}_1, \mathbf{R}_2, \dots) = \frac{1}{2} \sum_{ij} v_{I-I}(|\mathbf{R}_i - \mathbf{R}_j|) \quad (1.66)$$

where the sum is taken over all the ions, and we have implicitly assumed that the potential is dependent only on the distance between the ions. The positions of the ions in the lattice $\mathbf{R}_n^a = \mathbf{R}_n + \boldsymbol{\tau}_a$ are now interpreted as the equilibrium positions of the potential in Eq. (1.66), whereas the actual positions are given by

$$\mathbf{R}_n^a(t) = \mathbf{R}_n^a + \delta\mathbf{R}_n^a(t) = \mathbf{R}_n^a + \boldsymbol{\xi}_{n,a}(t) \quad (1.67)$$

Expanding (1.66) in a Taylor series up to the second order, we can treat the system in the harmonic approximation.

$$V_{I-I}(\mathbf{R}_1, \mathbf{R}_2, \dots) \simeq \frac{1}{2} \sum_{\alpha\alpha'} \sum_{m,m'} \frac{\partial^2 V_{I-I}}{\partial \xi_m^\alpha \partial \xi_{m'}^{\alpha'}} \xi_m^\alpha \xi_{m'}^{\alpha'} \quad (1.68)$$

where $\alpha = (x, y, z)$ and $m = (n, a)$. In this form, the Hamiltonian

$$H_{I-I}(\mathbf{R}_1, \mathbf{R}_2, \dots) = \sum_{n,a} \frac{(\mathbf{p}_n^a)^2}{2m_a} + V_{I-I}(\mathbf{R}_1, \mathbf{R}_2, \dots) \quad (1.69)$$

is not separable. Making a canonical change of coordinate from the position space to the reciprocal space, we can decouple the Hamiltonian into a sum of non-interacting Hamiltonians

$$H_{I-I} = \sum_{\mathbf{q}} H_{\mathbf{q}} \quad (1.70)$$

where \mathbf{q} is a vector in the reciprocal space. A detailed analysis shows that, for a crystal with r atoms per unit cell in d dimensions, the ionic Hamiltonian can be expressed as

$$\hat{H}_{ph} = \sum_{\lambda\mathbf{q}} \hbar\omega_{\lambda\mathbf{q}} \left(\hat{b}_{\lambda\mathbf{q}}^\dagger \hat{b}_{\lambda\mathbf{q}} + \frac{1}{2} \right) \quad (1.71)$$

where \mathbf{q} is a wavevector, $\lambda = (0, 1, \dots, rd)$ a branch index, $\omega_{\lambda\mathbf{q}}$ eigenfrequencies and \hat{b}^\dagger and \hat{b} creation and annihilation operators. Thus, the vibrational modes can be interpreted as a collection of bosonic quasi-particles of momentum \mathbf{q} and frequency $\omega_{\lambda\mathbf{q}}$. We call these quasi-particles phonons.

The system has a non-zero energy ground state

$$E_0 = \sum_{\lambda\mathbf{q}} \frac{1}{2} \hbar\omega_{\lambda\mathbf{q}} \quad (1.72)$$

The relation between the displacement in the real space $\delta\mathbf{R}_n^a$ and the creation and annihilation operators in the momentum space is

$$\delta\mathbf{R}_n^a = \sum_{\mathbf{q}\lambda} A_{\mathbf{q}\lambda}^a \hat{e}_{\mathbf{q}\lambda}^a e^{i\mathbf{q}\cdot\mathbf{R}_n^a} (\hat{b}_{\mathbf{q}\lambda} + \hat{b}_{-\mathbf{q}\lambda}^\dagger) \quad (1.73)$$

where $\hat{\epsilon}_{q\lambda}^a$ is the polarization vector and

$$A_{q\lambda}^a = \sqrt{\frac{\hbar}{2M_a N \omega_{q\lambda}}} \quad (1.74)$$

where M_a is mass of the a^{th} atom and N the number of atoms. The polarization vector $\hat{\epsilon}_{q\lambda}^a$ is used to describe the direction of the displacement δR_n^a with respect to the direction of propagation q . We have transversal phonons if $q \cdot \hat{\epsilon}_{q\lambda}^a = 0$ and longitudinal phonons if $q \times \hat{\epsilon}_{q\lambda}^a = 0$

1.2.5 Electron-phonon interaction

Now that we have described electrons and phonons, we can investigate how they interact with each other [18, 19]. Their interaction is of vital importance in solid state physics, polarons included. Our discussion starts with a periodic potential

$$V(\mathbf{r}, t) = \sum_{n,a} V_a(\mathbf{r} - \mathbf{R}_n^a(t)) \quad (1.75)$$

perturbed from its equilibrium position. $\mathbf{R}_n^a(t)$ is the position of the ions, and it is given by Eq. (1.67):

$$\mathbf{R}_n^a(t) = \mathbf{R}_n^a + \delta \mathbf{R}_n^a(t) \quad (1.76)$$

For typical vibrations, it can be shown that the displacements $\xi = |\delta \mathbf{R}_n^a(t)|$ are much smaller than the atomic spacing l . In particular

$$\frac{\xi}{l} \simeq \left[\frac{m}{M} \right]^{\frac{1}{4}} \quad (1.77)$$

and

$$\frac{E_{\text{ph}}}{E_{\text{el}}} \simeq \left(\frac{m}{M} \right)^{\frac{1}{2}} \quad (1.78)$$

where E_{ph} and E_{el} are respectively the phonon and electron energies, m is the electron mass and M the atomic mass. Given this scaling considerations, we can assume that the general band structure of the crystal remains the same. However, the interaction with the phonons can slightly modify it.

Using the assumption of small displacements, we can expand the potential in Eq. (1.75) in a Taylor series.

$$V(\mathbf{r}, t) = \sum_{n,a} V_a(\mathbf{r} - \mathbf{R}_n^a - \delta \mathbf{R}_n^a(t)) \simeq \sum_{n,a} [V_a(\mathbf{r} - \mathbf{R}_n^a) + \delta \mathbf{R}_n^a(t) \cdot \nabla_{\mathbf{r}} V_a(\mathbf{r} - \mathbf{R}_n^a)] \quad (1.79)$$

Terms of higher orders take into account anharmonic oscillations, which were already neglected in the study of phonons. The term $V_a(\mathbf{r} - \mathbf{R}_n^a)$ does not depend on the

deviation of the ions from their equilibrium positions. In fact, it is exactly the static periodic potential considered in the study of electrons in Section 1.2.2.

The total Hamiltonian of the system can be written as the sum of three terms

$$\hat{H} = \hat{H}_{\text{el}} + \hat{H}_{\text{ph}} + \hat{H}_{\text{el-ph}} \quad (1.80)$$

where \hat{H}_{el} and \hat{H}_{ph} are respectively the electrons and phonons Hamiltonians, given by Eq. (1.50) and Eq. (1.71). The term $\hat{H}_{\text{el-ph}}$ describes the electron-phonon interaction contribution, and it can be identified with

$$\hat{H}_{\text{el-ph}} = \sum_{n,a} \delta \mathbf{R}_n^a(t) \cdot \nabla_{\mathbf{r}} V_a(\mathbf{r} - \mathbf{R}_n^a) \quad (1.81)$$

We can use Eq. (1.73) to express the displacements in phonon coordinates

$$\hat{H}_{\text{el-ph}} = \sum_a \sum_{q\lambda} A_{q\lambda}^a \hat{\epsilon}_{q\lambda}^a \cdot \left(\sum_n e^{i\mathbf{q}\cdot\mathbf{R}_n^a} \cdot \nabla_{\mathbf{r}} V_a(\mathbf{r} - \mathbf{R}_n^a) \right) (\hat{b}_{q\lambda} + \hat{b}_{-q\lambda}^\dagger) \quad (1.82)$$

where $A_{q\lambda}^a$ is given by Eq. (1.74), $\hat{\epsilon}_{q\lambda}^a$ is the polarization vector, \mathbf{q} is the momentum of the phonon and $\hat{b}_{-q\lambda}^\dagger$ and $\hat{b}_{q\lambda}$ are the phonon creation and annihilation operators.

The electron part of the previous expression is still written in the language of first quantization. Using Eq. (1.36), we can express it in a second-quantized form. Suppressing the band indices and using the extended zone scheme, so that \mathbf{k}' and \mathbf{k} are not limited to the first Brillouin zone,

$$\hat{H}_{\text{el-ph}} = \sum_{\mathbf{k}'\mathbf{k}} \langle \mathbf{k}' | \hat{H}_{\text{el-ph}} | \mathbf{k} \rangle \hat{c}_{\mathbf{k}'}^\dagger \hat{c}_{\mathbf{k}} = \sum_{\mathbf{k}'\mathbf{k}} \sum_{\mathbf{q}\lambda} M_{\mathbf{k} \rightarrow \mathbf{k}'}^\lambda(\mathbf{q}) \hat{c}_{\mathbf{k}'}^\dagger \hat{c}_{\mathbf{k}} (\hat{b}_{\mathbf{q}\lambda} + \hat{b}_{-\mathbf{q}\lambda}^\dagger) \quad (1.83)$$

where the electron-phonon matrix M can be derived from Eq. (1.82). The previous expression can be interpreted as the transition of an electron from the state $|\mathbf{k}\rangle$ to the state $|\mathbf{k}'\rangle$ with either the creation of a phonon of momentum $-\mathbf{q}$ or the annihilation of a phonon of momentum \mathbf{q} . The matrix element $M_{\mathbf{k} \rightarrow \mathbf{k}'}^\lambda(\mathbf{q})$ gives the mechanical amplitude of such a process.

In order to evaluate M , we need to compute $\langle \mathbf{k}' | \hat{H}_{\text{el-ph}} | \mathbf{k} \rangle$. We start with a Fourier transform of the potential

$$V(\mathbf{r}) = \sum_{\mathbf{q}} V_a(\mathbf{q}) e^{i\mathbf{q}\cdot\mathbf{r}} \quad (1.84)$$

where $V_a(\mathbf{q})$ is the atomic form factor, and it is given by

$$V_a(\mathbf{q}) = \frac{1}{\Omega_a} \int e^{-i\mathbf{q}\cdot\mathbf{r}} V_a(\mathbf{r}) d\mathbf{r} = \frac{wN}{\Omega} \int e^{-i\mathbf{q}\cdot\mathbf{r}} V_a(\mathbf{r}) d\mathbf{r} \quad (1.85)$$

where Ω_a is the volume of a unit cell, Ω the volume of the crystal, N the number of unit cells and w the number of atoms per unit cell. We compute the gradient of the potential $\nabla_{\mathbf{r}} V_a(\mathbf{r})$ expressed as a Fourier series, and we evaluate it at $\mathbf{r} - \mathbf{R}_n^a$:

$$\nabla_{\mathbf{r}} V_a(\mathbf{r} - \mathbf{R}_n^a) = \frac{i}{wN} \sum_{\mathbf{q}'} \mathbf{q}' e^{i\mathbf{q}'\cdot\mathbf{r}} V_a(\mathbf{r}) e^{-i\mathbf{q}'\cdot\mathbf{R}_n^a} \quad (1.86)$$

Equation (1.82) can now be rewritten using Eq. (1.86) as

$$\hat{H}_{\text{el-ph}} = \frac{i}{wN} \sum_{\lambda} \sum_{q q'} A_{q\lambda}^a \hat{\epsilon}_{q\lambda}^a \cdot q' e^{iq' \cdot r} e^{i(q-q') \cdot R_n^a} V_a(q') (\hat{b}_{q\lambda} + \hat{b}_{-q\lambda}^\dagger) \quad (1.87)$$

We know that

$$\sum_n e^{i(q-q') \cdot R_n^a} = N \delta(q - q' + G) \quad (1.88)$$

where G is a vector of the reciprocal lattice. Then, most of the terms of the previous expression are zero, and we obtain

$$\begin{aligned} & \langle k' | \hat{H}_{\text{el-ph}} | k \rangle \\ &= \frac{i}{w} \sum_{a\lambda q} A_{q\lambda}^a \sum_G e^{-iG \cdot \tau_a} V_a(q+G) \hat{\epsilon}_{q\lambda}^a \cdot (q+G) (\hat{b}_{q\lambda} + \hat{b}_{-q\lambda}^\dagger) \langle k' | e^{i(q+G) \cdot r} | k \rangle \end{aligned} \quad (1.89)$$

where we have used that $G \cdot R_n = 2\pi n$, with n integer, to simplify the sum over λ . Finally, inserting this result in Eq. (1.89), we obtain an expression for the matrix element

$$M_{k \rightarrow k'}^\lambda(q) = \frac{i}{w} \sum_{aG} \sqrt{\frac{\hbar}{2M_a N \omega_{q\lambda}}} e^{-iG \cdot \tau_a} V_a(q+G) \hat{\epsilon}_{q\lambda}^a \cdot (q+G) \langle k' | e^{i(q+G) \cdot r} | k \rangle \quad (1.90)$$

We can compute the matrix element for a simple case where the initial and final state of the electron are plane waves. In this case,

$$\langle k' | e^{i(q+G) \cdot r} | k \rangle = \delta_{k', k+q+G} \quad (1.91)$$

and

$$M_{k \rightarrow k'}^\lambda(q) = \frac{i}{w} \sum_{aG} \sqrt{\frac{\hbar}{2M_a N \omega_{q\lambda}}} e^{-iG \cdot \tau_a} V_a(q+G) \hat{\epsilon}_{q\lambda}^a \cdot (q+G) \delta_{k', k+q+G} \quad (1.92)$$

The scattering process that we have explained earlier is now more clear. An electron of momentum $\hbar k$ is scattered in an electron of momentum $\hbar(k+q+G)$ by the emission of a phonon of momentum $-q$ or the absorption of a phonon of momentum q . We can identify two processes: the normal process, where $G = 0$, and the umklapp process, where $G \neq 0$. In the normal process $k' = k+q$, and assuming $w = 1$,

$$M_{k \rightarrow k+q}^\lambda(q) = i \sqrt{\frac{\hbar}{2M_a N \omega_{q\lambda}}} V_a(q) \hat{\epsilon}_{q\lambda} \cdot q \quad (1.93)$$

It is clear that in this type of process, only longitudinal phonons contribute to the scattering, since for transversal phonons $\hat{\epsilon}_{q\lambda} \cdot q = 0$.

The electrons are affected by deformations of the lattice in several ways [20]. The main effects of the coupling between electrons and phonons are:

- the scattering of electrons from a state \mathbf{k} to a state \mathbf{k}' , resulting in electrical resistivity;
- the absorption or creation of phonons;
- the creation of an attractive force between electrons, which is essential to explain superconductivity.

Another consequence is that electrons, moving in the lattice, carry a lattice polarization field with them. The particle resulting from the combination of the electron and the polarization field is called *polaron*, and it has a larger effective mass than the electron alone. In the next chapter, and in the rest of the thesis, we will focus on this last type of interaction.

2

THE POLARON PROBLEM

In this chapter, we describe and compare different models that have been proposed for the description of polarons. We start by reviewing the Landau-Pekar model, the first to be proposed and the simplest one. Then, Fröhlich and Holstein models are discussed as well. These two models are currently used for the description of large and small polarons, respectively. A comparison of the properties of small and large polarons is presented in the last section.

2.1 LANDAU-PEKAR MODEL

In the Landau-Pekar model, the electron is described by a wavefunction $\Psi(\mathbf{r})$ moving in a dielectric continuum medium. The static potential of the crystal is inserted in the model associating to the electron an effective mass m^* (see Section 1.2.2). In a polarizable material, the energy of the system is given by the kinetic energy of the electron plus the energy of the electromagnetic field

$$E = \frac{\hbar^2}{2m^*} \int d\mathbf{r} |\nabla \Psi(\mathbf{r})|^2 + \frac{1}{2} \int d\mathbf{r} \mathbf{E} \cdot \mathbf{D} \quad (2.1)$$

where \mathbf{D} can be expressed, using the Gauss law, as $\nabla \cdot \mathbf{D} = \rho = -e|\Psi(\mathbf{r})|^2$, or equivalently

$$\mathbf{D} = -\frac{e}{4\pi} \nabla \int d\mathbf{r}' \frac{|\Psi(\mathbf{r}')|^2}{|\mathbf{r} - \mathbf{r}'|} \quad (2.2)$$

For a dielectric medium, $\mathbf{D} = \epsilon_0 \epsilon^0 \mathbf{E}$, where ϵ_0 is the vacuum permittivity and ϵ^0 is the static dielectric constant. The electrostatic energy is then given by

$$\frac{1}{2} \int d\mathbf{r} \mathbf{E} \cdot \mathbf{D} = \frac{1}{2} \frac{1}{4\pi\epsilon_0} \frac{e^2}{\epsilon^0} \int d\mathbf{r} d\mathbf{r}' \frac{|\Psi(\mathbf{r})|^2 |\Psi(\mathbf{r}')|^2}{|\mathbf{r} - \mathbf{r}'|} \quad (2.3)$$

In the previous expression, \mathbf{E} includes contributions from both the displacement of the ions and the electric screening of the electrons. The latter effect is already taken into account by the electron effective mass, so we have to remove its contribution. Since the ions have a much larger mass than the electrons, they will not contribute to the high-frequency dielectric constant ϵ^∞ . The contribution of the electrons, that we want to remove, is then expressed by ϵ^∞ . Subtracting the contribution of the electrons from Eq. (2.3), we obtain

$$\frac{1}{2} \int d\mathbf{r} \mathbf{E} \cdot \mathbf{D} = \frac{1}{2} \frac{e^2}{4\pi\epsilon_0} \left(\frac{1}{\epsilon^0} - \frac{1}{\epsilon^\infty} \right) \int d\mathbf{r} d\mathbf{r}' \frac{|\Psi(\mathbf{r})|^2 |\Psi(\mathbf{r}')|^2}{|\mathbf{r} - \mathbf{r}'|} \quad (2.4)$$

If we define $1/\kappa = 1/\epsilon^\infty - 1/\epsilon^0$, we can rewrite the total energy as a functional of ψ

$$E[\psi] = \frac{\hbar^2}{2m^*} \int d\mathbf{r} |\nabla \psi(\mathbf{r})|^2 - \frac{1}{2} \frac{e^2}{4\pi\epsilon_0} \frac{1}{\kappa} \int d\mathbf{r} d\mathbf{r}' \frac{|\psi(\mathbf{r})|^2 |\psi(\mathbf{r}')|^2}{|\mathbf{r} - \mathbf{r}'|} \quad (2.5)$$

Following a variational approach, this functional can be minimized to find the polaron ground state energy. To do so, we must include a normalization constraint. This is done with the help of a Lagrange multiplier ε

$$\begin{aligned} E[\psi, \varepsilon] = & \frac{\hbar^2}{2m^*} \int d\mathbf{r} |\nabla \psi(\mathbf{r})|^2 - \frac{1}{2} \frac{e^2}{4\pi\epsilon_0} \frac{1}{\kappa} \int d\mathbf{r}' \frac{|\psi(\mathbf{r})|^2 |\psi(\mathbf{r}')|^2}{|\mathbf{r} - \mathbf{r}'|} \\ & - \varepsilon \left(\int d\mathbf{r} |\psi(\mathbf{r})|^2 - 1 \right) \end{aligned} \quad (2.6)$$

Minimizing with respect to ψ^* and ε , we obtain a Schrödinger-type equation

$$\left(-\frac{\hbar^2}{2m^*} \nabla^2 - \frac{e^2}{4\pi\epsilon_0} \frac{1}{\kappa} \int d\mathbf{r}' \frac{|\psi(\mathbf{r}')|^2}{|\mathbf{r} - \mathbf{r}'|} \right) \psi(\mathbf{r}) = \varepsilon \psi(\mathbf{r}) \quad (2.7)$$

The Lagrange multiplier ε has the dimension of an energy, but it is not exactly the polaron ground state energy. Projecting Eq. (2.7) onto ψ^* and confronting the result with Eq. (2.6), we obtain the ground state energy E_0

$$E_0 = \varepsilon + \frac{1}{2} \frac{e^2}{4\pi\epsilon_0} \frac{1}{\kappa} \int d\mathbf{r}' \frac{|\psi(\mathbf{r})|^2 |\psi(\mathbf{r}')|^2}{|\mathbf{r} - \mathbf{r}'|} \quad (2.8)$$

Equation (2.7) is not known to have an exact solution. However, we can solve it variationally using a trial wavefunction $(\pi r_p^3)^{-1/2} e^{-r/r_p}$ and minimizing E with respect to r_p . As in the hydrogen atom, the kinetic term minimization favours larger r_p (delocalized states) and the potential term favours smaller r_p (localized states). Performing the minimization, the polaron radius r_p , is found to be

$$r_p = \frac{16}{5} \frac{\kappa}{m^*/m_e} a_0 \quad (2.9)$$

where m_e is the mass of the electron and a_0 the Bohr radius [21]. The value of the ground state energy is

$$E_0 = -\frac{50}{512} \alpha^2 \hbar \omega_{LO} \quad (2.10)$$

where ω_{LO} is the characteristic frequency of longitudinal optical phonon and

$$\alpha = \frac{e^2}{4\pi\epsilon_0 \hbar} \sqrt{\frac{m^*}{2\hbar\omega_{LO}}} \frac{1}{\kappa} \quad (2.11)$$

is the coupling constant

Despite its simplicity, the Landau-Pekar model provides simple formulas for the polaron ground state, radius and effective mass [4]. However, to have polaron bound states, κ must be positive, which implies $\epsilon^0 > \epsilon^\infty$. This is true only for polar crystals, but polarons are observed in non-polar crystals as well. Moreover, this model carries an intrinsic contradiction. Treating the medium as a continuum requires the polaron to be large, but formally justified results can only be obtained in the strong coupling regime, a situation improbable for real materials.

2.2 FRÖHLICH POLARONS

We have anticipated in Section 2.1 a simple model for the description of polarons. To improve that first model, we have to describe the mechanics of the lattice polarization more precisely. In this section, we discuss the Fröhlich Hamiltonian, derived by Fröhlich in 1950 [5]. This Hamiltonian is appropriate for the description of large polarons in ionic crystals and polar semiconductors. In these materials, we expect electrons to interact strongly with longitudinal optical phonons. The interaction is mediated by the electric field produced by the polarization of the lattice. The contribution of transversal phonons is expected to be negligible because of the smaller electric field they produce.

2.2.1 Derivation of the Fröhlich Hamiltonian

In this section we derive the Fröhlich Hamiltonian following the approach described by Kittel [20]. We assume the longitudinal phonons to be dispersionless (with frequency ω_{LO}) and we treat the polarizable medium as a continuum.

In an ionic crystal, the polarization \mathbf{P} can be considered as the sum of two components: the optical polarization \mathbf{P}_o and the infra-red polarization \mathbf{P}_{ir} . The former is due to the displacement of bound electrons, and it is characterized by a resonance frequency in the optical or ultraviolet region; the latter is due to the displacement of ions and its resonance frequency is in the infra-red region. Given the slow velocities of the electrons that we are going to consider, the optical polarization is always excited at its static value. Thus, given the absence of a dependence on the velocity of the electron, the optical polarization \mathbf{P}_o is of no interest to us, since it does not modify the energy of the electron between different states. On the other hand, this does not apply to the infra-red polarization, because of its lower resonance frequency. At long distances from the electric charge (placed at \mathbf{r}_0), \mathbf{P}_{ir} can be obtained subtracting the optical polarization \mathbf{P}_o from the total polarization \mathbf{P} . Thus, it can be derived from an electric potential $V(\mathbf{r})$ by

$$4\pi\mathbf{P}_{\text{ir}}(\mathbf{r}) = \nabla V(\mathbf{r}) \quad (2.12)$$

where

$$V(\mathbf{r}) = -\frac{1}{\kappa} \frac{e}{|\mathbf{r} - \mathbf{r}_0|} \quad (2.13)$$

with $1/\kappa = 1/\epsilon^\infty - 1/\epsilon^0$. As in the Landau-Pekar model, the contribution of the lattice to the dielectric constant (κ) is obtained by removing the contribution of the electrons (ϵ^∞) from the static dielectric constant (ϵ^0).

The infra-red polarization is proportional to the amplitude of the displacement of the ions. Generalizing Eq. (1.73), for a generic point \mathbf{r} , we can express the displacement in the point \mathbf{r} as

$$\xi(\mathbf{r}) = \sum_{\mathbf{q}} A \hat{\epsilon}_{\mathbf{q}} e^{i\mathbf{q} \cdot \mathbf{r}} (\hat{b}_{\mathbf{q}} + \hat{b}_{-\mathbf{q}}^\dagger) \quad (2.14)$$

where we have dropped the indices a and λ because we are considering atoms of the same mass and phonons of the same branch. Moreover, A does not depend on \mathbf{q} because the phonons are assumed to be dispersionless. Since we are considering only longitudinal phonons, the polarization vector $\hat{\epsilon}_{\mathbf{q}}$ must be parallel to \mathbf{q} . However, we cannot simply suppose $\hat{\epsilon}_{\mathbf{q}} = \hat{q}$. In fact, we have to guarantee that $\xi(\mathbf{r})$ is real:

$$\xi^\dagger(\mathbf{r}) = \sum_{\mathbf{q}} A \hat{\epsilon}_{\mathbf{q}}^\dagger e^{-i\mathbf{q} \cdot \mathbf{r}} (\hat{b}_{\mathbf{q}}^\dagger + \hat{b}_{-\mathbf{q}}) = \sum_{\mathbf{q}} A \hat{\epsilon}_{-\mathbf{q}}^\dagger e^{i\mathbf{q} \cdot \mathbf{r}} (\hat{b}_{\mathbf{q}} + \hat{b}_{-\mathbf{q}}^\dagger) = \xi(\mathbf{r}) \quad (2.15)$$

This implies $\hat{\epsilon}_{\mathbf{q}}^\dagger = \hat{\epsilon}_{-\mathbf{q}}$, and then $\hat{\epsilon}_{\mathbf{q}} = i\hat{q}$.

As we anticipated, P_{ir} is proportional to the amplitude of the displacement

$$P_{ir} = F \xi(\mathbf{r}) = iF \sum_{\mathbf{q}} A \hat{q} e^{i\mathbf{q} \cdot \mathbf{r}} (\hat{b}_{\mathbf{q}} + \hat{b}_{-\mathbf{q}}^\dagger) \quad (2.16)$$

where F is a constant to be determined. We expand the electric potential in a Fourier series

$$V(\mathbf{r}) = \sum_{\mathbf{q}} V(\mathbf{q}) e^{i\mathbf{q} \cdot \mathbf{r}} \quad (2.17)$$

and we compute the gradient

$$\nabla V(\mathbf{r}) = i \sum_{\mathbf{q}} \mathbf{q} V(\mathbf{q}) e^{i\mathbf{q} \cdot \mathbf{r}} \quad (2.18)$$

Using Eq. (2.12) and comparing Eq. (2.16) with Eq. (2.18), we find

$$V(\mathbf{q}) = 4\pi \frac{FA}{q} (\hat{b}_{\mathbf{q}} + \hat{b}_{-\mathbf{q}}^\dagger) \quad (2.19)$$

We want to express the constant F in terms of the interaction energy of two electrons in a polarizable material of dielectric constant ϵ . We consider two electrons completely localized in two points \mathbf{r}_1 and \mathbf{r}_2 . The electrons will interact directly through the vacuum electric field and indirectly through a perturbation induced by the optical

phonon field. The interaction Hamiltonian is given by the sum of the potential of the two electrons

$$\begin{aligned} H_{\text{el-el}} &= -eV(\mathbf{r}_1) - eV(\mathbf{r}_2) = 4\pi eFA \sum_{\mathbf{q}} q^{-1} (e^{i\mathbf{q}\cdot\mathbf{r}_1} + e^{i\mathbf{q}\cdot\mathbf{r}_2})(\hat{b}_{\mathbf{q}} + \hat{b}_{-\mathbf{q}}^\dagger) \\ &= 4\pi eFA \sum_{\mathbf{q}} q^{-1} [\hat{b}_{\mathbf{q}}(e^{i\mathbf{q}\cdot\mathbf{r}_1} + e^{i\mathbf{q}\cdot\mathbf{r}_2}) + \hat{b}_{\mathbf{q}}^\dagger(e^{-i\mathbf{q}\cdot\mathbf{r}_1} + e^{-i\mathbf{q}\cdot\mathbf{r}_2})] \end{aligned} \quad (2.20)$$

where in the second line we have changed the sign of \mathbf{q} in the second term, using the fact that the sum is taken over all \mathbf{q} . The second-order energy perturbation caused by the previous Hamiltonian is given by

$$\Delta E = - \sum_{\mathbf{q}} \frac{\langle 0 | H_{\text{el-el}} | \mathbf{q} \rangle \langle \mathbf{q} | H_{\text{el-el}} | 0 \rangle}{\hbar\omega_{\text{LO}}} \quad (2.21)$$

where $|0\rangle$ and $|\mathbf{q}\rangle$ are respectively states with no phonons and a single LO phonon in the state \mathbf{q} with energy $\hbar\omega_{\text{LO}}$. Inserting Eq. (2.20) in the previous expression and dropping the terms with \mathbf{r}_1 and \mathbf{r}_2 alone, which are self-energy terms,

$$\begin{aligned} \Delta E &= -2 \sum_{\mathbf{q}} \frac{\langle 0 | eV(\mathbf{r}_1) | \mathbf{q} \rangle \langle \mathbf{q} | eV(\mathbf{r}_2) | 0 \rangle}{\hbar\omega_{\text{LO}}} \\ &= -2 \frac{(4\pi eFA)^2}{\hbar\omega_{\text{LO}}} \sum_{\mathbf{q}} q^{-2} \langle 0 | e^{i\mathbf{q}\cdot\mathbf{r}_1} (\hat{b}_{\mathbf{q}} + \hat{b}_{\mathbf{q}}^\dagger) | \mathbf{q} \rangle \langle \mathbf{q} | e^{-i\mathbf{q}\cdot\mathbf{r}_2} (\hat{b}_{\mathbf{q}} + \hat{b}_{\mathbf{q}}^\dagger) | 0 \rangle \\ &= -2 \frac{(4\pi eFA)^2}{\hbar\omega_{\text{LO}}} \sum_{\mathbf{q}} q^{-2} \langle \mathbf{q} | e^{i\mathbf{q}\cdot\mathbf{r}_1} | \mathbf{q} \rangle \langle \mathbf{q} | e^{-i\mathbf{q}\cdot\mathbf{r}_2} | \mathbf{q} \rangle \\ &= -2 \frac{(4\pi eFA)^2}{\hbar\omega_{\text{LO}}} \sum_{\mathbf{q}} \frac{e^{i\mathbf{q}\cdot(\mathbf{r}_1-\mathbf{r}_2)}}{q^2} \end{aligned} \quad (2.22)$$

Knowing that, when summed over all \mathbf{q} ,

$$\sum_{\mathbf{q}} \frac{4\pi}{q^2} e^{i\mathbf{q}\cdot\mathbf{r}} = \Omega \frac{1}{|\mathbf{r}|} \quad (2.23)$$

where Ω is the volume of the region of interest, we can rewrite the perturbation energy as

$$\Delta E = - \frac{8\pi\Omega A^2 F^2}{\hbar\omega_{\text{LO}}} \frac{e^2}{|\mathbf{r}_1 - \mathbf{r}_2|} \quad (2.24)$$

The form of this interaction is exactly the same of an attractive Coulomb potential between two charges placed at \mathbf{r}_1 and \mathbf{r}_2 . The origin of this attraction is the polarization of the ions of the medium. Thus, the factor

$$- \frac{8\pi\Omega A^2 F^2}{\hbar\omega_{\text{LO}}} \quad (2.25)$$

gives exactly the contribution of the ions to the dielectric constant. Since the static dielectric constant ϵ^0 includes both the contribution of the ions and of the electrons, and the high-frequency dielectric constant ϵ^∞ only the contribution of the electrons, we can express Eq. (2.25) as

$$\frac{1}{\epsilon^0} = \frac{1}{\epsilon^\infty} - \frac{8\pi\Omega A^2 F^2}{\hbar\omega_{LO}} \quad (2.26)$$

The electric potential is then given by

$$V(\mathbf{r}) = \sum_{\mathbf{q}} V(\mathbf{q}) e^{i\mathbf{q}\cdot\mathbf{r}} = \sum_{\mathbf{q}} \left[\frac{2\pi e^2 \hbar \omega_{LO}}{\Omega q^2} \left(\frac{1}{\epsilon^\infty} - \frac{1}{\epsilon^0} \right) \right]^{1/2} (\hat{b}_{\mathbf{q}} + \hat{b}_{-\mathbf{q}}^\dagger) e^{i\mathbf{q}\cdot\mathbf{r}} \quad (2.27)$$

and writing it in a fully second-quantized form, we find

$$\hat{H}_{el-ph} = \sum_{\mathbf{k}'\mathbf{k}} \sum_{\mathbf{q}} \left[\frac{2\pi e^2 \hbar \omega_{LO}}{\Omega q^2} \left(\frac{1}{\epsilon^\infty} - \frac{1}{\epsilon^0} \right) \right]^{1/2} \langle \mathbf{k}' | e^{i\mathbf{q}\cdot\mathbf{r}} | \mathbf{k} \rangle (\hat{b}_{\mathbf{q}\lambda} + \hat{b}_{-\mathbf{q}\lambda}^\dagger) \hat{c}_{\mathbf{k}'}^\dagger \hat{c}_{\mathbf{k}} \quad (2.28)$$

Confronting the previous expression with Eq. (1.83), we can identify the interaction matrix

$$M_{\mathbf{k}-\mathbf{q} \rightarrow \mathbf{k}} = \left[\frac{2\pi e^2 \hbar \omega_{LO}}{\Omega q^2} \left(\frac{1}{\epsilon^\infty} - \frac{1}{\epsilon^0} \right) \right]^{1/2} \quad (2.29)$$

which is more commonly written as

$$M_{\mathbf{q}} = \frac{\hbar \omega_{LO}}{|q|} \left(\frac{\hbar}{2m\omega_{LO}} \right)^{1/4} \left(\frac{4\pi\alpha}{\Omega} \right)^{1/2} \quad (2.30)$$

where α is the dimensionless Fröhlich coupling constant, defined as

$$\alpha = \frac{e^2}{\hbar} \left(\frac{1}{\epsilon^\infty} - \frac{1}{\epsilon^0} \right) \sqrt{\frac{m}{2\hbar\omega_{LO}}} \quad (2.31)$$

where m is the electron band mass.

Adding the electrons and phonons contributions, and approximating the wavefunctions of the electrons to plane waves as we did in Eq. (1.91), we can write the Fröhlich Hamiltonian as

$$\begin{aligned} H_{Fröhlich} = & \sum_{\mathbf{k}} \frac{\hbar^2 k^2}{2m} + \sum_{\mathbf{q}} \hbar \omega_{LO} \left(\hat{b}_{\mathbf{q}}^\dagger \hat{b}_{\mathbf{q}} + \frac{1}{2} \right) \\ & + \sum_{\mathbf{k}\mathbf{q}} \frac{\hbar \omega_{LO}}{|q|} \left(\frac{\hbar}{2m\omega_{LO}} \right)^{1/4} \left(\frac{4\pi\alpha}{\Omega} \right)^{1/2} \hat{c}_{\mathbf{k}}^\dagger \hat{c}_{\mathbf{k}-\mathbf{q}} (\hat{b}_{\mathbf{q}} + \hat{b}_{-\mathbf{q}}^\dagger) \end{aligned} \quad (2.32)$$

The interaction of the electrons with the lattice described by Eq. (2.32) has multiple effects. Some consequences we may expect are:

- The electron band energy is decreased, because part of the energy is used to produce phonons.
- The effective mass of the electron is increased, because the electron has to deform the lattice while moving, carrying the deformation with itself.
- The mobility of the electron is modified, because the polaron experiences scattering effects different from the ones of a free electron.

We can analyse quantitatively the first of these two effects using approximation techniques. We will do it in the next two sections, applying perturbation theory and variational methods to the Fröhlich Hamiltonian.

2.2.2 Weak coupling limit

Polarons are often divided in two classes: large and small. The name is due to their effective radius r_p , which is defined as the effective radius of the polarized area. If r_p is greater than the interatomic distance l , the polaron is said to be large; on the contrary, if $r_p \lesssim l$, the polaron is said to be small. In the former case, the coupling is usually weak ($\alpha < 1$), in the latter it is strong ($\alpha > 1$). In the weak-coupling regime, it is possible to use perturbation theory to derive some properties of large polarons.

The total Hamiltonian is

$$\begin{aligned}\hat{H} &= \hat{H}_{\text{el}} + \hat{H}_{\text{ph}} + \hat{H}_{\text{el-ph}} \\ &= \sum_{\mathbf{k}} \frac{\hbar^2 \mathbf{k}^2}{2m} + \sum_{\mathbf{q}} \hbar \omega_{\text{LO}} \left(\hat{b}_{\mathbf{q}}^\dagger \hat{b}_{\mathbf{q}} + \frac{1}{2} \right) + \sum_{\mathbf{k}, \mathbf{q}} M_{\mathbf{q}} \hat{c}_{\mathbf{k}}^\dagger \hat{c}_{\mathbf{k}-\mathbf{q}} (\hat{b}_{\mathbf{q}} + \hat{b}_{-\mathbf{q}}^\dagger)\end{aligned}\quad (2.33)$$

where $M_{\mathbf{q}}$ is given by Eq. (2.30)

$$M_{\mathbf{q}} = \frac{\hbar \omega_{\text{LO}}}{|\mathbf{q}|} \left(\frac{\hbar}{2m \omega_{\text{LO}}} \right)^{1/4} \left(\frac{4\pi\alpha}{\Omega} \right)^{1/2} \quad (2.34)$$

and it is supposed to be small ($\alpha < 1$). The unperturbed Hamiltonian

$$\hat{H}^{(0)} = \hat{H}_{\text{el}} + \hat{H}_{\text{ph}} \quad (2.35)$$

has plane waves $|\mathbf{k}\rangle$ as eigenfunctions of the single electron part and many-body basis kets $|n_1 \dots n_q \dots\rangle$ as eigenfunctions of the phonon part. The full eigenkets are given by the composition of the two parts $|\mathbf{k}; \{n_q\}\rangle = |\mathbf{k}\rangle |n_1 \dots n_q \dots\rangle$. The energy of this state is

$$E_{\mathbf{k}, \{n_q\}}^{(0)} = \frac{\hbar^2 \mathbf{k}^2}{2m} + \hbar \omega_{\text{LO}} \sum n_q \quad (2.36)$$

and the ground state is given by an electron with $\mathbf{k} = 0$ and the vacuum state $|0\rangle$ for the phonon part. First-order perturbation theory results in no energy shift, since

$$\langle \mathbf{k} | \langle 0 | (\hat{b}_{\mathbf{q}} + \hat{b}_{-\mathbf{q}}^\dagger) | 0 \rangle | \mathbf{k} \rangle = 0 \quad (2.37)$$

Going to second order

$$\Delta E_{\mathbf{k}}^{(2)} = \sum_{\alpha \neq \{\mathbf{k}; 0\}} \frac{|\langle \mathbf{k}; 0 | \hat{H}_{\text{el-ph}} | \alpha \rangle|^2}{E_{\{\mathbf{k}; 0\}} - E_{\alpha}} = \sum_{\alpha \neq \{\mathbf{k}; 0\}} \frac{|\langle \mathbf{k}; 0 | M_{\mathbf{q}} \hat{c}_{\mathbf{k}}^{\dagger} \hat{c}_{\mathbf{k}-\mathbf{q}} (\hat{b}_{\mathbf{q}} + \hat{b}_{-\mathbf{q}}^{\dagger}) | \alpha \rangle|^2}{E_{\{\mathbf{k}; 0\}} - E_{\alpha}} \quad (2.38)$$

where $|\alpha\rangle$ is an excited state. The only states that contribute with non-null terms are states composed of an electron and a single phonon of wavevector \mathbf{q} . The electron is scattered by the phonon in a state of wavevector $\mathbf{k} - \mathbf{q}$, so that the total momentum is conserved. The kets $|\alpha\rangle$ are thus of the form $|\mathbf{k} - \mathbf{q}; n_{\mathbf{q}} = 1\rangle$, with energy

$$E_{\alpha} = \frac{\hbar^2}{2m}(\mathbf{k} - \mathbf{q})^2 + \hbar\omega_{\text{LO}} = \frac{\hbar^2\mathbf{k}^2}{2m} - \frac{\hbar^2\mathbf{k} \cdot \mathbf{q}}{m} + \frac{\hbar^2\mathbf{q}^2}{2m} + \hbar\omega_{\text{LO}} \quad (2.39)$$

The shift in the energy is then

$$\Delta E_{\mathbf{k}} = - \sum_{\mathbf{q}} \frac{|M_{\mathbf{q}}|^2}{\hbar\omega_{\text{LO}} + \frac{\hbar^2}{2m}\mathbf{q}^2 - \frac{\hbar^2}{m}\mathbf{k} \cdot \mathbf{q}} \quad (2.40)$$

We may denote

$$|M_{\mathbf{q}}|^2 = \frac{C}{\mathbf{q}^2} \quad (2.41)$$

where

$$C = (\hbar\omega_{\text{LO}})^2 \left(\frac{\hbar}{2m\omega_{\text{LO}}} \right)^{1/2} \left(\frac{4\pi\alpha}{\Omega} \right) \quad (2.42)$$

Defining $\mu = \frac{\mathbf{k} \cdot \mathbf{q}}{|\mathbf{k}| |\mathbf{q}|}$, we can convert the sum in Eq. (2.40) in an integral,

$$\sum_{\mathbf{q}} \rightarrow \frac{\Omega}{(2\pi)^3} \int d\mathbf{q} = \frac{\Omega}{(2\pi)^3} \int 2\pi q^2 dq d\mu \quad (2.43)$$

then,

$$\Delta E_{\mathbf{k}} = - \frac{\Omega}{(2\pi)^2} \int_{-1}^1 d\mu \int_0^{q_{\text{BZ}}} dq \frac{C}{\hbar\omega_{\text{LO}} + \frac{\hbar^2}{2m}q^2 - \frac{\hbar^2}{m}kq\mu} \quad (2.44)$$

where the integral is extended until the boundary of the first Brillouin zone. Although the integral in Eq. (2.44) may be exactly solved, we can gain some insights on the main physical meaning by developing it in powers of k and letting $q_{\text{BZ}} \rightarrow \infty$. Choosing an appropriate set of units, so that $\hbar = \omega_{\text{LO}} = 2m = 1$,

$$\Delta E_{\mathbf{k}} = - \frac{\alpha}{\pi} \left[2 \int_0^\infty dq \frac{1}{1+q^2} + 4k^2 \int_{-1}^1 d\mu \int_0^\infty dq \frac{q^2\mu^2}{(1+q^2)^3} \right] = -\alpha - \frac{\alpha}{6}k^2 \quad (2.45)$$

and plugging back the standard units,

$$\Delta E_{\mathbf{k}} = -\alpha\hbar\omega_{\text{LO}} - \frac{\alpha}{6} \frac{\hbar^2}{2m} k^2 \quad (2.46)$$

Finally, the perturbed energy is

$$E_{\mathbf{k}} = -\alpha \hbar \omega_{\text{LO}} + \left(1 - \frac{\alpha}{6}\right) \frac{\hbar^2}{2m} \mathbf{k}^2 \quad (2.47)$$

where the factor on the right can be interpreted as an electron with a new effective mass $m^* = m/(1 - \alpha/6)$. The band energy is shifted down by an overall factor of $\alpha \hbar \omega_{\text{LO}}$ and the effective mass of the electron is increased. This is a reasonable conclusion: the electron digs itself a hole in the lattice potential, lowering its energy, and it has to carry the deformation along its path, resulting in a bigger effective mass.

It is also possible to compute the average number of phonons coupled with the electron at $T = 0$ K. The phonon number operator is given by

$$\hat{N}_{\text{ph}} = \sum_{\mathbf{q}} \hat{b}_{\mathbf{q}}^\dagger \hat{b}_{\mathbf{q}} \quad (2.48)$$

so its average value is

$$\langle \hat{N}_{\text{ph}} \rangle = \sum_{\mathbf{q}} \langle \psi | \hat{b}_{\mathbf{q}}^\dagger \hat{b}_{\mathbf{q}} | \psi \rangle \quad (2.49)$$

where $|\psi\rangle$ is the electron-phonon ket. The ket can be expanded near a state with no phonons $|\mathbf{k}, 0\rangle$

$$|\psi_{\mathbf{k}}\rangle = |\mathbf{k}, 0\rangle + |\delta\psi_{\mathbf{k}}\rangle \quad (2.50)$$

where $|\delta\psi_{\mathbf{k}}\rangle$ is the variation of the wavefunction due to the electron-phonons interaction. Using first-order perturbation theory, it can be found that

$$|\delta\psi_{\mathbf{k}}\rangle = \sum_{a \neq \{\mathbf{k}, 0\}} |a\rangle \frac{\langle \mathbf{k}; 0 | \hat{H}_{\text{el-ph}} | a \rangle}{E_{\{\mathbf{k}, 0\}} - E_a} = \sum_{\mathbf{q}} |\mathbf{k} - \mathbf{q}; n_{\mathbf{q}} = 1\rangle \frac{M_{\mathbf{q}}}{E_{\{\mathbf{k}, 0\}} - E_{\{\mathbf{k} - \mathbf{q}, n_{\mathbf{q}} = 1\}}} \quad (2.51)$$

Inserting the result in Eq. (2.49), we obtain

$$\langle \hat{N}_{\text{ph}} \rangle = \sum_{\mathbf{q}} \frac{\langle \mathbf{k} - \mathbf{q}; n_{\mathbf{q}} = 1 | \hat{b}_{\mathbf{q}}^\dagger \hat{b}_{\mathbf{q}} | \mathbf{k} - \mathbf{q}; n_{\mathbf{q}} = 1 \rangle}{(\hbar \omega_{\text{LO}} + \frac{\hbar^2}{2m} \mathbf{q}^2 - \frac{\hbar^2}{m} \mathbf{k} \cdot \mathbf{q})^2} |M_{\mathbf{q}}|^2 \quad (2.52)$$

and substituting q and μ as before,

$$\langle \hat{N}_{\text{ph}} \rangle = \sum_{\mathbf{q}} \frac{|M_{\mathbf{q}}|^2}{(\hbar \omega_{\text{LO}} + \frac{\hbar^2}{2m} \mathbf{q}^2 - \frac{\hbar^2}{m} \mathbf{k} \cdot \mathbf{q} \mu)^2} \quad (2.53)$$

or, expressed in our usual set of units,

$$\langle \hat{N}_{\text{ph}} \rangle = \sum_{\mathbf{q}} \frac{|M_{\mathbf{q}}|^2}{(1 + q^2 - \frac{kq}{2} \mu)^2} \quad (2.54)$$

Converting the sum into an integral, inserting Eq. (2.34), and expanding to the lowest order in k , we find

$$\langle \hat{N}_{\text{ph}} \rangle = \frac{\Omega}{(2\pi)^2} \frac{4\pi\alpha}{\Omega} \int_0^\infty \frac{4\pi}{(1+q^2)^2} dq = \frac{\alpha}{2} \quad (2.55)$$

The meaning of the parameter α is now more clear: it is a measure of the number of phonons coupled with the electron.

2.2.3 Strong coupling limit

In the strong coupling regime, perturbation theory cannot be applied. However, it is possible to use a different approximation method: variational analysis. When the coupling is strong, we expect the electron to dig itself a deeper hole in the lattice potential. The electron will then localize inside the hole. In this regime, we can suppose the polaron wavefunction to be composed of two factors: an unknown phonon wavefunction $|\phi_{\text{ph}}\rangle$ and an electron wavefunction $|\psi_{\text{el}}\rangle$. The latter is assumed to have the shape of a Gaussian

$$\psi(\mathbf{r}) = \frac{1}{r_p^{3/2}} e^{-\frac{r^2}{2r_p^2}} \quad (2.56)$$

where r_p is the effective radius of the polaron, which we use as variational parameter. According to variational theory, we have to minimize the functional

$$\langle \phi_{\text{ph}} | \langle \psi_{\text{el}} | \hat{H} | \psi_{\text{el}} \rangle | \phi_{\text{ph}} \rangle \quad (2.57)$$

where \hat{H} is the Fröhlich Hamiltonian

$$\hat{H} = \sum_k \frac{\hbar^2 k^2}{2m} + \sum_q \hbar\omega_{\text{LO}} \left(\hat{b}_q^\dagger \hat{b}_q + \frac{1}{2} \right) + \sum_q M_q e^{iq \cdot r} (\hat{b}_q + \hat{b}_{-q}^\dagger) \quad (2.58)$$

and M_q is the usual interaction matrix given in Eq. (2.34). In the natural units introduced in the previous section, the Hamiltonian becomes

$$\hat{H} = \sum_k k^2 + \sum_q \left(\hat{b}_q^\dagger \hat{b}_q + \frac{1}{2} \right) + \sum_q M_q e^{iq \cdot r} (\hat{b}_q + \hat{b}_{-q}^\dagger) \quad (2.59)$$

Defining the kinetic energy

$$E_{\text{kin}} = \langle \psi_{\text{el}} | \mathbf{k}^2 | \psi_{\text{el}} \rangle = \frac{3}{2r_p^2} \quad (2.60)$$

and the electron density

$$\rho_q = \langle \psi_{\text{el}} | e^{iq \cdot r} | \psi_{\text{el}} \rangle = e^{-q^2 r_p^2 / 4} \quad (2.61)$$

we find

$$\langle \Psi_{\text{el}} | \hat{H} | \Psi_{\text{el}} \rangle = E_{\text{kin}} + \sum_{\mathbf{q}} \left[\hat{b}_{\mathbf{q}}^\dagger \hat{b}_{\mathbf{q}} + \frac{1}{2} + M_{\mathbf{q}} \rho_{\mathbf{q}} \hat{b}_{\mathbf{q}} + M_{\mathbf{q}}^* \rho_{\mathbf{q}}^* \hat{b}_{\mathbf{q}}^\dagger \right] \quad (2.62)$$

Ignoring the phonon ground state energy and completing the square, we find

$$\langle \Psi_{\text{el}} | \hat{H} | \Psi_{\text{el}} \rangle = E_{\text{kin}} + \sum_{\mathbf{q}} \left(\hat{b}_{\mathbf{q}}^\dagger + M_{\mathbf{q}} \rho_{\mathbf{q}} \right) \left(\hat{b}_{\mathbf{q}} + M_{\mathbf{q}}^* \rho_{\mathbf{q}}^* \right) - \sum_{\mathbf{q}} |M_{\mathbf{q}} \rho_{\mathbf{q}}|^2 \quad (2.63)$$

The second term is easily understandable as a displaced harmonic oscillator. The equilibrium position is shifted from zero to $-M_{\mathbf{q}} \rho_{\mathbf{q}}$. This is precisely the effect of the polarization induced by the electron. It is clear that the minimum of the functional will correspond to the vacuum state of the displaced harmonic oscillator. In this state, the energy is simply

$$E_{\text{var}} = \langle \Psi_{\text{el}} | \hat{H} | \Psi_{\text{el}} \rangle = E_{\text{kin}} - \sum_{\mathbf{q}} |M_{\mathbf{q}} \rho_{\mathbf{q}}|^2 \quad (2.64)$$

Converting the sum to an integral, integrating over the angular part, and inserting Eqs. (2.34) and (2.61), the second term becomes

$$\sum_{\mathbf{q}} |M_{\mathbf{q}} \rho_{\mathbf{q}}|^2 \simeq \frac{\Omega}{(2\pi)^3} \int_0^\infty 4\pi q^2 \frac{C}{q^2} e^{-q^2 r_p^2/2} dq = \sqrt{\frac{2}{\pi}} \frac{\alpha}{r_p} \quad (2.65)$$

Thus, inserting Eqs. (2.60) and (2.65) in Eq. (2.64), the variational energy is

$$E_{\text{var}} = \frac{3}{2r_p^2} - \sqrt{\frac{2}{\pi}} \frac{\alpha}{r_p} \quad (2.66)$$

and it is minimized for

$$r_p = \sqrt{\frac{\pi}{2}} \frac{3}{\alpha} \quad (2.67)$$

Plugging back the standard units, the final energy is

$$E_{\text{var}} = -\frac{\alpha^2}{3\pi} \hbar\omega_{\text{LO}} \quad (2.68)$$

If we confront it with the result obtained in Eq. (2.47) using perturbation theory, we see that, for the ground state, the dependence on α is proportional to $-\alpha^2$ instead of $-\alpha$. The variational energy is then lower than the perturbation energy for large α , which is the region of validity of the assumptions we made.

2.3 HOLSTEIN POLARONS

Holstein proposed a different Hamiltonian to model polarons. The main difference is in how the lattice is treated. Instead of working with a continuum, polarizable medium

like Fröhlich, Holstein took into account the discreteness of the lattice. The model is based on the tight-binding model, which was briefly introduced in Section 1.2.3. In the next sections, we will use it to derive the Holstein Hamiltonian for a 1D system, and solve it in the weak coupling limit.

2.3.1 Derivation of the Holstein Hamiltonian

To simplify the derivation, we consider a linear chain of N atoms. At equilibrium, the atom n is placed at the position $R_n = na$, where a is the lattice constant. The atoms are allowed to move, and their interaction energy is given by the harmonic oscillator approximation. The Hamiltonian of the lattice is then

$$\hat{H}_{\text{I-I}} = \sum_n \left(\frac{P_n^2}{2M} + \frac{1}{2} M \omega_0^2 x_n^2 \right) \quad (2.69)$$

where P_n is the momentum of the n^{th} atom, x_n the separation between the atoms n and $n+1$ and M their mass.

The electrons are allowed to interact with the lattice through a potential

$$U = \sum_n U(r - R_n, x_n) \quad (2.70)$$

where r is the position of the electron. The key feature of this model is that U depends on the interatomic separation x_n . This results in the coupling of the electrons with the lattice vibrations, so with phonons. Adding the electron kinetic energy term, the total Hamiltonian is given by

$$\hat{H} = \sum_n \left(-\frac{\hbar^2}{2M} \frac{\partial^2}{\partial x_n^2} + \frac{1}{2} M \omega_0^2 x_n^2 \right) - \frac{\hbar^2}{2m} \frac{\partial^2}{\partial r^2} + \sum_n U(r - R_n, x_n) \quad (2.71)$$

Following the tight-binding approach described in Section 1.2.3, we express the electrons wavefunctions as a linear combination of the single atomic orbitals

$$\psi(r) = \sum_n \alpha_n(x_1 \dots x_N) \phi_n(r - na, x_n) \quad (2.72)$$

where α_n are complex coefficients and ϕ_n are the solutions of the corresponding Schrödinger equations

$$\left[-\frac{\hbar^2}{2m} \frac{\partial^2}{\partial r^2} + U(r - na, x_n) \right] \phi_n = E_n(x_n) \phi_n \quad (2.73)$$

This results in a differential equation for the coefficients α_n , which is obtained through a standard projection procedure. The full calculation can be found in the Appendix of the original Holstein paper [6]. We only report the result

$$\left[i\hbar \frac{\partial}{\partial t} - \sum_p \left(-\frac{\hbar^2}{2M} \frac{\partial^2}{\partial x_p^2} + \frac{1}{2} M \omega_0^2 x_p^2 \right) - E(x_n) - W_n(x_1 \dots x_N) \right] \alpha_n(x_1 \dots x_N) = \sum_{(\pm)} J(x_n, x_{n+1}) \alpha_{n\pm 1}(x_1 \dots x_N) \quad (2.74)$$

where

$$W_n(x_1 \dots x_N) = \int |\phi_n(r - na, x_n)|^2 \sum_{p \neq n} U(r - pa, x_p) dr \quad (2.75)$$

$$J(x_n, x_m) = \int \phi_n^*(r - na, x_n) U(r - na, x_n) \phi(r - ma, x_m) dr \quad (2.76)$$

We can simplify Eq. (2.74) introducing three approximations:

1. The neglect of the energies $W_n(x_1 \dots x_N)$.
2. The neglect of the x -dependance of J . The function $J(x_n, x_m)$ reduces to a constant $-J$, which can also be denominated $-t$. It corresponds to the parameter t introduced in the tight-binding approximation in Eq. (1.61).
3. The x -dependance of the energy $E_n(x_n)$ is taken to be linear: $E_n(x_n) = -Ax_n$

The physical meaning of the first approximation (1) is to neglect the perturbation of the wavefunction localized on the site n caused by the interaction with other sites p . This assumption is reasonable in the tight-binding model that we are employing. The result is that the expectation value of the energy of an electron is only dependent on one coordinate x_n , the one of the site where the electron is localized.

With the previous simplifications, Eq. (2.74) becomes

$$i\hbar \frac{\partial}{\partial t} \alpha_n = \sum_p \left(-\frac{\hbar^2}{2M} \frac{\partial^2}{\partial x_p^2} + \frac{1}{2} M \omega_0^2 x_p^2 \right) \alpha_n - t(\alpha_{n+1} + \alpha_{n-1}) \alpha_n - Ax_n \alpha_n \quad (2.77)$$

A study of Eq. (2.77) in its current form is presented by Holstein in his paper [6]. However, we will follow a different approach, expressing it in the second-quantization formalism. From now on, we also consider again a 3D system, generalizing the results that we obtain for the 1D one.

The first term of Eq. (2.77) is exactly the lattice interaction term we have already encountered in Eq. (1.69). In the momentum space, its second-quantized form is

given by Eq. (1.71). For a single phonon branch in 3D, assuming the phonons to be dispersionless and optical as we did for the Fröhlich Hamiltonian, we find

$$\hat{H}_{\text{ph}} = \hbar\omega_0 \sum_{\mathbf{q}} \left(\hat{b}_{\mathbf{q}}^\dagger \hat{b}_{\mathbf{q}} + \frac{1}{2} \right) \quad (2.78)$$

The second term is the tight-binding energy encountered in Section 1.2.3 and its second-quantized form is given by Eq. (1.64)

$$\hat{H}_{\text{el}} = \sum_{\mathbf{k}} \epsilon_{\mathbf{k}}^{\text{tb}} \hat{c}_{\mathbf{k}}^\dagger \hat{c}_{\mathbf{k}} \quad (2.79)$$

Finally, the last term is responsible for the electron-phonon interaction energy. We have seen that, for a normal scattering process, the general form of the interaction matrix is given by Eq. (1.93). Since in this case the interaction amplitude is independent of the momentum, we can write the interaction matrix as constant g in the position space and g/\sqrt{N} in the momentum space. The interaction Hamiltonian is then given by Eq. (1.83)

$$\hat{H}_{\text{el-ph}} = \frac{g}{\sqrt{N}} \sum_{\mathbf{k}, \mathbf{q}} \hat{c}_{\mathbf{k}+\mathbf{q}}^\dagger \hat{c}_{\mathbf{k}} (\hat{b}_{-\mathbf{q}}^\dagger + \hat{b}_{\mathbf{q}}) \quad (2.80)$$

The final Holstein Hamiltonian is

$$\hat{H}_{\text{Holstein}} = \sum_{\mathbf{k}} \epsilon_{\mathbf{k}}^{\text{tb}} \hat{c}_{\mathbf{k}}^\dagger \hat{c}_{\mathbf{k}} + \hbar\omega_0 \sum_{\mathbf{q}} \left(\hat{b}_{\mathbf{q}}^\dagger \hat{b}_{\mathbf{q}} + \frac{1}{2} \right) + \frac{g}{\sqrt{N}} \sum_{\mathbf{k}, \mathbf{q}} \hat{c}_{\mathbf{k}+\mathbf{q}}^\dagger \hat{c}_{\mathbf{k}} (\hat{b}_{-\mathbf{q}}^\dagger + \hat{b}_{\mathbf{q}}) \quad (2.81)$$

2.3.2 Weak coupling limit

Like the Fröhlich Hamiltonian, the Holstein Hamiltonian is not exactly solvable in its general form. Although it is exactly solvable for a two state system [22], we will use perturbation theory to find an approximate solution. We will follow the same procedure we adopted in Section 2.2.2. This method is valid as long as the coupling constant

$$\alpha = \frac{g^2}{d\hbar\omega_0 t} \quad (2.82)$$

is small, where d is the dimensionality of the problem.

We start by splitting the Holstein Hamiltonian in an unperturbed term $\hat{H}^{(0)} = \hat{H}_{\text{el}} + \hat{H}_{\text{ph}}$ and the perturbation $\hat{H}_{\text{el-ph}}$. The solution to the unperturbed problem is found solving the Hamiltonian

$$\hat{H}^{(0)} = \sum_{\mathbf{k}} \epsilon_{\mathbf{k}}^{\text{tb}} \hat{c}_{\mathbf{k}}^\dagger \hat{c}_{\mathbf{k}} + \hbar\omega_0 \sum_{\mathbf{q}} \left(\hat{b}_{\mathbf{q}}^\dagger \hat{b}_{\mathbf{q}} \right) \quad (2.83)$$

where we have ignored the ground-state phonon energy and where

$$\epsilon_{\mathbf{k}}^{\text{tb}} = -t \sum_{\delta} \cos(\mathbf{k} \cdot \mathbf{R}_{\delta}) \quad (2.84)$$

where δ is the index of the nearest neighbours. Working in one dimension, considering a linear chain of atoms separated by a unitary distance, Eq. (2.84) reduces to

$$\epsilon_k^{tb} = -2t \cos(k) \quad (2.85)$$

where the factor two arises from the fact that there are two nearest neighbours for each ion. If we separate the polaron ket in its electron and phonon part $|k, n_q\rangle = |k\rangle |n_1 \dots n_q \dots\rangle$ we can find its unperturbed energy

$$E_{k,n_q}^{(0)} = -t \sum_{\delta} \cos(k) + \hbar\omega_0 \sum_q n_q \quad (2.86)$$

We are now ready to add the perturbation

$$\hat{H}_{el-ph} = \frac{g}{\sqrt{N}} \sum_{k,q} \hat{c}_{k+q}^{\dagger} \hat{c}_k (\hat{b}_{-q}^{\dagger} + \hat{b}_q) \quad (2.87)$$

The form of this Hamiltonian is totally analogous to the Fröhlich Hamiltonian we have encountered in Section 2.2.2, with $\frac{g}{\sqrt{N}}$ in place of M_q . With analogous considerations, we can then conclude that the only states that give rise to non-null terms in the second-order energy correction

$$\Delta E_k^{(2)} = \sum_{a \neq \{k;0\}} \frac{|\langle k;0 | \hat{H}_{el-ph} | a \rangle|^2}{E_{\{k;0\}} - E_a} = \frac{g^2}{N} \sum_{a \neq \{k;0\}} \frac{|\langle k;0 | \hat{c}_k^{\dagger} \hat{c}_{k-q} (\hat{b}_q + \hat{b}_{-q}) | a \rangle|^2}{E_{\{k;0\}} - E_a} \quad (2.88)$$

are states with an electron of momentum $k - q$ and a single phonon of momentum q . Using Eq. (2.85) we can find the energy of the ground state

$$E_{k,0}^{(0)} = -2t \cos(k) \quad (2.89)$$

and of the excited state

$$E_a = E_{k,n_q=1}^{(0)} = -2t \cos(k - q) + \hbar\omega_0 \quad (2.90)$$

Plugging Eqs. (2.89) and (2.90) in Eq. (2.88) and replacing the sum with an integral as we did in Section 2.2.2, we find

$$\begin{aligned} \Delta E_k &= -\frac{1}{2\pi} \int dq \frac{g^2}{2t \cos(k) + 2t \cos(k - q) - \hbar\omega_0} \\ &= -\frac{1}{2\pi} \int dq \frac{\alpha \hbar\omega_0 t}{2t \cos(k) + 2t \cos(k - q) - \hbar\omega_0} \end{aligned} \quad (2.91)$$

The total energy is then

$$E_k = -2t \cos(k) - \frac{1}{2\pi} \int dq \frac{\alpha \hbar\omega_0 t}{2t \cos(k) + 2t \cos(k - q) - \hbar\omega_0} \quad (2.92)$$

2.4 SMALL AND LARGE POLARONS

In the previous sections, we have divided polarons in two categories: small and large. A small polaron is defined as a polaron that is created by a distortion of the lattice smaller than the unit cell. Conversely, a large polaron originates from a distortion bigger than the unit cell. The distinction can also be made in terms of the strength of the electron-phonon coupling. When it is strong, electrons are localized around a single atom and only the interactions with the nearest-neighbours atoms are relevant. When the interaction is weak, longer-range interactions becomes more significant. A picture of the charge isosurfaces of a small and large polaron is given in Fig. 2.1

We have seen how the two types of polarons are usually described by two different Hamiltonians. The Fröhlich Hamiltonian is typically used for large polarons, where the discreteness of the lattice plays a minor role. For this reason, large polarons are often also called Fröhlich polarons. On the other hand, small polarons - which are also called Holstein polarons - are described by the Holstein Hamiltonian, which takes into account the discrete behaviour of the lattice more accurately.

The differences between small and large polarons are more than just their sizes. A very important one is their mobility [23]. Polarons form in polarizable materials, such ionic crystals or polar semiconductors. In both cases, electronic transport occur via hopping. The charges are thermally activated over a gap, and hop from one site to another. However, if in semiconductors the charges must have enough energy to jump over the band gap, in polaronic materials the gap is much narrower. In fact, polarons have to jump from a localized state (the polaronic band) to the conduction band.

Several diffusion mechanisms have been identified to describe polarons mobility. However, a simplified picture can be drawn to highlight the general differences between small and large polarons [24]. Small polarons typically hop from one site to another assisted by phonons, when the distortion of the polaron's site is disturbed by thermal vibrations. The resulting motion is thus incoherent, and the mobility is usually much smaller than $1 \text{ cm}^2 \text{V}^{-1} \text{s}^{-1}$. The mobility increases with temperature, since this increases the thermal vibrations which cause the hopping. Conversely, large polarons tend to follow a quasi-free-carrier-like motion. We have seen that the effective mass is greater for polarons than for free-charges. The large effective mass prevents them from scattering with the phonon field, and this results in a higher mobility. The mobility is reduced by the increasing of temperature, which makes the scattering more effective.

The property of small and large polarons discussed above are summarized in Table 2.1.

Tabella 2.1: Summary of small and large polarons properties. The table is taken from Franchini's review on polarons [24]

Small (Holstein) polarons	Large (Fröhlich) polarons
$\hat{H}_{\text{el-ph}} = \frac{g}{\sqrt{N}} \sum_{\mathbf{k}, \mathbf{q}} \hat{c}_{\mathbf{k}+\mathbf{q}}^\dagger \hat{c}_{\mathbf{k}} (\hat{b}_{-\mathbf{q}}^\dagger + \hat{b}_{\mathbf{q}})$	$\hat{H}_{\text{el-ph}} = \sum_{\mathbf{k}, \mathbf{q}} M_{\mathbf{q}} \hat{c}_{\mathbf{k}+\mathbf{q}}^\dagger \hat{c}_{\mathbf{k}} (\hat{b}_{\mathbf{q}} + \hat{b}_{-\mathbf{q}}^\dagger)$
<ul style="list-style-type: none"> Short-range electron-phonon interaction Polaron radius \approx lattice parameter Narrow mid-gap electronic state (≈ 1 eV below E_F) Incoherent motion (phonon assisted) Thermally activated hopping mobility $\ll 1 \text{ cm}^2 \text{V}^{-1} \text{s}^{-1}$ Mobility increasing with temperature 	<ul style="list-style-type: none"> Long-range electron-phonon interaction Polaron radius \gg lattice parameter Shallow mid-gap electronic state (≈ 10 meV below E_F) Coherent motion Free carrier mobility $\gg 1 \text{ cm}^2 \text{V}^{-1} \text{s}^{-1}$ Mobility decreasing with temperature

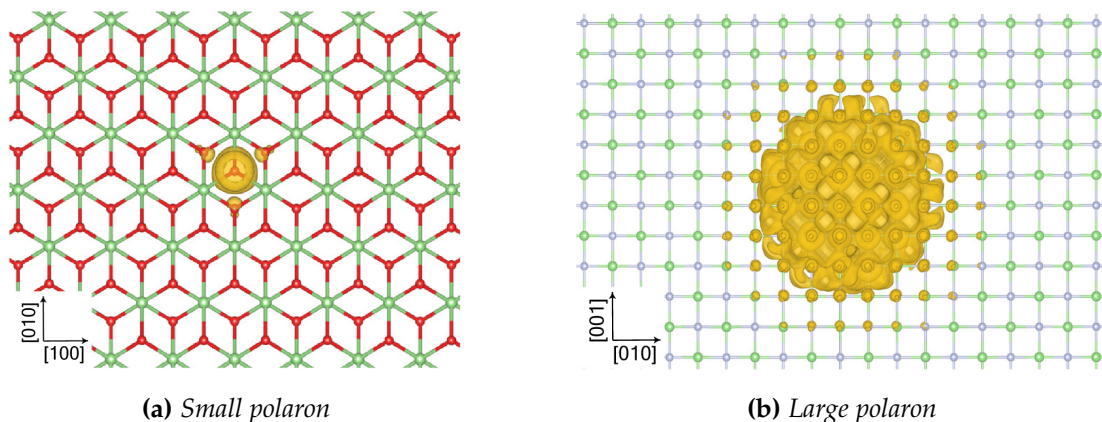


Figura 2.1: Example of charge isosurfaces of a small and a large polaron in a 2D lattice. The images are taken from Sio et al. [11]

3

DENSITY FUNCTIONAL THEORY

Condensed Matter Physics has to deal with systems of many interacting particles, typically electrons. We have already introduced a mathematical formalism that allows us to describe such systems. However, the resulting Hamiltonians do not usually have any analytical solution. In these cases, we must rely on numerical simulations. One particular approach has emerged as a popular choice in the last decades: DFT. DFT allows us to solve many-electrons problems in an *ab-initio* fashion. It is based on two seminal papers, written by Hohenberg and Kohn in 1964 [25] and Kohn and Sham in 1965 [26]. The key advantage of this formalism is that it provides a means to transform a many interacting electrons problem into an effective-field one-electron self-consistent problem, which is exact in principle. In the next sections, we will introduce this formalism and its implementation, focusing on VASP.

3.1 INTRODUCTION TO DFT

3.1.1 *Ground state and density functional formalism*

The basic assumption of DFT is that, for a system of interacting electrons in an external potential $v(\mathbf{r})$, the ground-state energy E_g can be expressed as a functional of the sole charge density $\rho(\mathbf{r})$. We will indicate this with the standard notation $E_g[\rho]$. This statement was proven for the first time by Hohenberg and Kohn in 1964 [25]. This allows to greatly simplify the problem of solving a many-body Schrödinger equation. In fact, the ground-state energy depends only on a single scalar field $\rho(\mathbf{r})$, whereas solving the Schrödinger equation would imply finding the multi-particle wavefunction $\Psi(\mathbf{r}_1 \dots \mathbf{r}_N)$.

We want to show that we can write E_g as a functional of $\rho(\mathbf{r})$. We will take the point of view that our problem is entirely determined by the external potential $v(\mathbf{r})$. In fact, for a system of electrons subject to an external potential $v(\mathbf{r})$, the Hamiltonian can be expressed as the sum of three components

$$\hat{H} = \sum_i v(\mathbf{r}_i) + \sum_i \frac{\mathbf{p}_i^2}{2m} + \frac{1}{2} \sum_{i \neq j} \frac{e^2}{|\mathbf{r}_i - \mathbf{r}_j|} = V + T + U \quad (3.1)$$

In a system of N electrons, the last two terms (T and U) are universal. The difference

between two systems, and so the solution Ψ , is entirely determined by the first term $V = \sum_i v(\mathbf{r}_i)$. If we define

$$\rho(\mathbf{r}) = \sum_i \langle \Psi | \delta^3(\mathbf{r} - \mathbf{r}_i) | \Psi \rangle \quad (3.2)$$

since Ψ is completely determined by V , ρ is also a unique functional of V . The main point of the theory is that the converse is also true. We can prove it by contradiction.

Let's assume that the contrary is true. That is, there exists another external potential $v'(\mathbf{r})$ such that the ground state solution of the respective Schrödinger equation $|\Psi'\rangle$ gives the same density $\rho'(\mathbf{r}) = \rho(\mathbf{r})$. The two potentials are assumed to differ for more than a constant. Since $|\Psi'\rangle$ and $|\Psi\rangle$ are solutions to Schrödinger equations with different potentials, they will differ for more than a phase factor. We know from variational theory that the ground-state wavefunction minimizes the expectation value of the Hamiltonian, so

$$E' = \langle \Psi' | H' | \Psi' \rangle < \langle \Psi | H' | \Psi \rangle \quad (3.3)$$

but

$$\langle \Psi | H' | \Psi \rangle = \langle \Psi | H - V + V' | \Psi \rangle = E + \int [v'(\mathbf{r}) - v(\mathbf{r})] \rho(\mathbf{r}) d\mathbf{r} \quad (3.4)$$

which leads to the inequality

$$E' < E + \int [v'(\mathbf{r}) - v(\mathbf{r})] \rho(\mathbf{r}) d\mathbf{r} \quad (3.5)$$

Similarly, for the primed system, we find

$$E < E' + \int [v(\mathbf{r}) - v'(\mathbf{r})] \rho'(\mathbf{r}) d\mathbf{r} \quad (3.6)$$

Adding the previous two equations, remembering that $\rho'(\mathbf{r}) = \rho(\mathbf{r})$, we get

$$E' + E < E + E' \quad (3.7)$$

which is obviously absurd. This proves that $v(\mathbf{r})$ is a unique functional of $\rho(\mathbf{r})$. In other words, given a physical electron density, there is a unique external potential that can produce it. In addition, since knowing $v(\mathbf{r})$ defines completely the problem, $|\Psi\rangle$ is also a functional of $\rho(\mathbf{r})$.

We can define a new functional

$$F[\rho] = \langle \Psi[\rho] | T + U | \Psi[\rho] \rangle \quad (3.8)$$

and, using Eq. (3.1), express the ground-state energy as

$$E_g[\rho] = \langle \Psi[\rho] | V + T + U | \Psi[\rho] \rangle = \int v(\mathbf{r}) \rho(\mathbf{r}) d\mathbf{r} + F[\rho] \quad (3.9)$$

where $v(\mathbf{r})$ is a functional of ρ . The problem is now reduced to minimizing the functional $E_g[\rho]$ with the constraint $N = \int \rho(\mathbf{r}) d\mathbf{r}$. If $F[\rho]$ had a simple known expression, the problem would be quite straight forward. Unfortunately, this is not the case, and the expression of $F[\rho]$ is not explicitly known.

3.1.2 The Kohn-Sham Equations

Kohn and Sham proved in 1965 that $\rho(\mathbf{r})$ can be determined solving a set of N Shrödinger-type equations, subject to an effective potential $v'(\mathbf{r})$. It is important to emphasize that the solutions to the N equations should not be interpreted as orbitals of the real system. In the Kohn-Sham formalism, two different systems are considered: the real system, made of N interacting particles subject to an external potential $v(\mathbf{r})$, and a fictitious system, made of N non-interacting particles subject to an effective potential $v'(\mathbf{r})$.

In the expression of the ground-state energy shown in Eq. (3.9), $F[\rho]$ contains both the kinetic energy T and the interaction energy U , for which there are no known expressions in terms of the density $\rho(\mathbf{r})$. However, we can estimate $F[\rho]$ in some limiting cases. If we neglect exchange and correlation effects, the interaction energy is given by the Hartree term

$$U_{KS} = \frac{e^2}{2} \int \frac{\rho(\mathbf{r})\rho(\mathbf{r}')}{|\mathbf{r}-\mathbf{r}'|} d\mathbf{r} d\mathbf{r}' \quad (3.10)$$

For a non-interacting system of N particles of density $\rho(\mathbf{r})$, where each particle is described by a wavefunction $\phi_i(\mathbf{r})$, the total kinetic energy is given by

$$T_{KS} = -\frac{\hbar^2}{2m} \sum_i \int \phi_i^*(\mathbf{r}) \nabla^2 \phi_i(\mathbf{r}) d\mathbf{r} \quad (3.11)$$

with

$$\rho(\mathbf{r}) = \sum_i \phi_i^*(\mathbf{r}) \phi_i(\mathbf{r}) \quad (3.12)$$

It is reasonable to expect that the interaction and kinetic energy of the real system will be close to the sum of Eq. (3.10) and Eq. (3.11). It is then convenient to write the functional $F[\rho]$ as

$$F[\rho] = T_{KS}[\rho] + U_{KS}[\rho] + E_{xc}[\rho] \quad (3.13)$$

where E_{xc} is added to take into account all the contributions to $F[\rho]$ that are not included in $T_{KS}[\rho]$ and $U_{KS}[\rho]$. Our entire ignorance on $F[\rho]$ is now contained in $E_{xc}[\rho]$. We can express the ground-state energy functional as

$$E_g[\rho] = \int v(\mathbf{r})\rho(\mathbf{r}) d\mathbf{r} + T_{KS} + \frac{e^2}{2} \int \frac{\rho(\mathbf{r})\rho(\mathbf{r}')}{|\mathbf{r}-\mathbf{r}'|} d\mathbf{r} d\mathbf{r}' + E_{xc}[\rho] \quad (3.14)$$

It is now time to bring in the fictitious systems we introduced above. Our goal is to determine a second system of N interacting particles with the same density $\rho(\mathbf{r})$ of the real system. The Schrödinger equation of the fictitious system are solved to determine $\rho(\mathbf{r})$. Then, the density is plugged in Eq. (3.14) to determine the value of the ground-state energy functional. Using the variational principle, the non-interacting system is varied to minimize the real system ground state energy. The minimum gives

us the charge density and the ground-state energy of the real system. The variation gives rise to a set of Euler-Lagrange equations that governs the single-particle orbitals and energies of the fictitious system.

Let's then consider a non-interacting system of N particles subject to an effective potential $v'(\mathbf{r})$. The density $\rho'(\mathbf{r})$ is determined solving

$$\left(-\frac{\hbar^2}{2m} \nabla^2 + v'(\mathbf{r}) \right) \phi_i(\mathbf{r}) = \epsilon_i \phi_i(\mathbf{r}) \quad (3.15)$$

and computing $\rho'(\mathbf{r}) = \sum_i |\phi_i(\mathbf{r})|^2$. The kinetic energy is then given by

$$T_{KS}[\rho'] = \sum_i \epsilon_i - \int v'(\mathbf{r}) \rho'(\mathbf{r}) d\mathbf{r} \quad (3.16)$$

Inserting this result in Eq. (3.14), we find an expression for the ground-state energy functional

$$\begin{aligned} E_g[\rho'] &= \int v(\mathbf{r}) \rho'(\mathbf{r}) d\mathbf{r} \\ &\quad + \left(\sum_i \epsilon_i - \int v'(\mathbf{r}) \rho'(\mathbf{r}) d\mathbf{r} \right) + \frac{e^2}{2} \int \frac{\rho'(\mathbf{r}) \rho'(\mathbf{r}')}{|\mathbf{r} - \mathbf{r}'|} d\mathbf{r} d\mathbf{r}' + E_{xc}[\rho'] \end{aligned} \quad (3.17)$$

To obtain the physical density and the actual ground-state energy, we minimize Eq. (3.17) by varying ρ' . That is, we evaluate the shift in energy $E_g \rightarrow E_g + \delta E_g$ after a variation $\rho' \rightarrow \rho' + \delta \rho'$

$$\begin{aligned} \delta E_g &= \int v(\mathbf{r}) \delta \rho'(\mathbf{r}) d\mathbf{r} + \sum_i \delta \epsilon_i - \int \delta \rho'(\mathbf{r}) \left[v'(\mathbf{r}) + \int \frac{\delta v'(\mathbf{r}')}{\delta \rho'(\mathbf{r}')} \rho'(\mathbf{r}') d\mathbf{r}' \right] d\mathbf{r} \\ &\quad + e^2 \int \delta \rho'(\mathbf{r}) \frac{\rho'(\mathbf{r}')}{|\mathbf{r} - \mathbf{r}'|} d\mathbf{r} d\mathbf{r}' + \int \delta \rho'(\mathbf{r}) \frac{\delta E_{xc}}{\delta \rho'(\mathbf{r})} d\mathbf{r} \\ &= \sum_i \delta \epsilon_i + \int \delta \rho'(\mathbf{r}) \left[v(\mathbf{r}) - v'(\mathbf{r}) - \int \frac{\delta v'(\mathbf{r}')}{\delta \rho'(\mathbf{r})} \rho'(\mathbf{r}') d\mathbf{r}' + e^2 \int \frac{\rho'(\mathbf{r}')}{|\mathbf{r} - \mathbf{r}'|} d\mathbf{r}' + \frac{\delta E_{xc}}{\delta \rho'(\mathbf{r})} \right] d\mathbf{r} \end{aligned} \quad (3.18)$$

When $\rho'(\mathbf{r})$ minimizes the functional, the previous expression is equal to zero. Minimizing with respect to $\rho'(\mathbf{r})$ is equivalent to doing it with respect to $v'(\mathbf{r})$. Since, to first order in $\delta v'$,

$$\sum_i \delta \epsilon_i = \sum_i \langle \phi_i | \delta v' | \phi_i \rangle = \int \delta v'(\mathbf{r}') \rho'(\mathbf{r}') d\mathbf{r}' = \int \delta \rho'(\mathbf{r}) \frac{\delta v'(\mathbf{r}')}{\delta \rho'(\mathbf{r})} \rho'(\mathbf{r}') d\mathbf{r} d\mathbf{r}' \quad (3.19)$$

setting Eq. (3.18) equals to zero gives

$$v'(\mathbf{r}) = v(\mathbf{r}) + e^2 \int \frac{\rho'(\mathbf{r}')}{|\mathbf{r} - \mathbf{r}'|} d\mathbf{r}' + \frac{\delta E_{xc}}{\delta \rho'(\mathbf{r})} \quad (3.20)$$

The equations that govern the fictitious non-interacting system are then

$$\left(-\frac{\hbar^2}{2m} \nabla^2 + v(r) + v_H(r) + v_{xc}(r) \right) \phi_i(r) = \epsilon_i \phi_i(r) \quad (3.21)$$

where

$$v_H(r) = e^2 \int \frac{\rho'(\mathbf{r}')}{|\mathbf{r} - \mathbf{r}'|} d\mathbf{r}' \quad (3.22)$$

$$v_{xc}(r) = \frac{\delta E_{xc}}{\delta \rho'(\mathbf{r})} \quad (3.23)$$

and $\rho'(\mathbf{r})$ is given by

$$\rho'(\mathbf{r}) = \sum_i |\phi_i(\mathbf{r})|^2 \quad (3.24)$$

Equations 3.21 are known as Kohn-Sham equations. They look like a set of Schrödinger equations, but they are inherently different. In fact, the left-hand side (LHS) of the equations depends on ρ , and so on ϕ_i , like the right-hand side (RHS).

Given E_{xc} , the equations are solvable with a self-consistent calculation. In a self-consistent calculation, an initial $\rho(\mathbf{r})$ is assumed and the LHS of the equation is evaluated. Then, the equation is solved like a standard Schrödinger equation, and a new $\rho(\mathbf{r})$ is computed through Eq. (3.24). The solution is plugged in Eq. (3.17) to find the ground-state energy of the real system. The procedure is repeated with the new density, and it ends when the difference in energy between two successive steps is smaller than a pre-chosen value. It is important to emphasize that the coefficients ϵ_i have nothing to do with the energies of the electrons of the interacting system. The only quantities with physical meaning are the total electron density $\rho(\mathbf{r})$ and the ground-state energy E_g .

Since E_{xc} is not exactly known, different approximations have been developed. The different models are developed based on some constraints that the exchange-correlation functional must satisfy. The models are tested on simple systems that are exactly solvable, like the uniform electron gas. The functional are generally parametrized, and the parameters can be set based on *ab-initio* calculations or fitting experimental data.

A common approach is to write E_{xc} as

$$E_{xc} = \int \rho(\mathbf{r}) \epsilon_{xc}(\mathbf{r}) d\mathbf{r} \quad (3.25)$$

The functionals E_{xc} are generally divided in two classes: the local density approximation (LDA) and generalized gradient approximation (GGA). In LDA, $\epsilon_{xc}(\mathbf{r})$ is assumed to depend only on the density $\rho(\mathbf{r})$, whereas in GGA it is assumed to depend both on $\rho(\mathbf{r})$ and on its gradient $\nabla \rho(\mathbf{r})$. The functionals take the form

$$E_{xc}^{\text{LDA}} = \int \rho(\mathbf{r}) \epsilon_{xc}(\rho) d\mathbf{r} \quad (3.26)$$

$$E_{xc}^{\text{GGA}} = \int \rho(\mathbf{r}) \epsilon_{xc}(\rho, \nabla \rho) d\mathbf{r} \quad (3.27)$$

3.1.3 DFT corrections: DFT+U

DFT has a good accuracy when determining structural and cohesive properties, but it often fails in the prediction of electronic properties. The fundamental problem of DFT resides in the Hartree term

$$\frac{e^2}{2} \int \frac{\rho'(\mathbf{r})\rho'(\mathbf{r}')}{|\mathbf{r}-\mathbf{r}'|} d\mathbf{r}d\mathbf{r}' \quad (3.28)$$

In fact, this term does not exclude the contribution of self-interaction to the electronic repulsion energy. This effect cannot be counterbalanced by the exchange-correlation term, because the form of the two is inherently different. The Hartree term is given by a double integral, whereas the exchange-correlation energy is given by a single integral.

The result is that DFT favours delocalized states, which have lower self-interaction energy, over localized states. A well-known consequence is that band gaps energies of semiconductors are usually underestimated [27]. Many alternative solutions have been proposed, like the hybrid functionals and the post-Hartree-Fock methods [28]. However, we will focus on a solution proposed by Anisimov, called DFT+U [29]. This approach has the advantage to be as reliable as the other methods, but with significantly lower computational cost.

The development of DFT+U was inspired by another model: the Hubbard model. This model is useful to describe the transition between conducting and isolating systems. It is based on the tight-binding approximation: the electrons are described by the usual atomic orbitals and are allowed to "jump" from one atom to the other. The probability of the jump is described by a transfer integral t . The Hubbard model adds to the tight-binding model an on-site repulsion, consequence of the repulsion of the electrons residing in the same orbital. In its simpler formulation, the Hubbard model can be applied to a linear chain of hydrogen atoms. The electrons occupy s orbitals and may have spin up or down. This system can be described by the following Hubbard Hamiltonian

$$\hat{H}_{\text{Hub}} = -t \sum_{\langle i,j \rangle} \hat{c}_{j,\sigma}^\dagger \hat{c}_{j,\sigma} + U \sum_i \hat{N}_{i\uparrow} \hat{N}_{i\downarrow} \quad (3.29)$$

where $\langle i,j \rangle$ indicates two nearest-neighbours atoms, σ is the spin, \hat{c}^\dagger and \hat{c} the creation and annihilation operators and \hat{N} the number operator. The first term is parametrized by the transfer integral t , which represents the energy of the electron that jumps between the atoms. The second term takes into account the potential energy given by the repulsion of the electrons. The first term favours delocalized states, whereas the second one tends to localize the electrons.

The original DFT Hamiltonian is corrected adding the Hubbard contribution. This is not done for all the electrons, but only for the electrons that reside in the most localized orbitals (d and f). Electrons in s and p orbitals are treated with standard DFT. This method was simplified by Dudarev et al. in 1998 [30]. In their model, the intra-atomic self-interaction error is corrected via a Hubbard-like model which depends only on

the difference $U - t$. The parameters t and U are usually determined semi-empirically, fitting the data from the experimental band gaps, or from first principles using methods like the constrained random phase approximation (cRPA) [31]. The final effect of using a DFT+U approach instead of doing a standard DFT calculation is the broadening of the band gap. The greater the value assigned to U is, the more the states are localized and the more the gap broadens.

3.2 IMPLEMENTATION

We are now interested in how the theory that we have presented is implemented in simulation programs. DFT is widely used for simulating several systems, from atoms to crystals. However, it is mainly employed in the study of solid state systems. The main reason is that in crystals, we can take advantage of the symmetries of the system to simplify the computation. We have shown in Section 1.2.1 that crystals are periodic systems, where the periodicity is described by the lattice vectors \mathbf{R}_n . Every property, included the ion potential, shares the same periodicity. The central consequence is that the solutions to the Schrödinger equation for this kind of potential can be written in a Bloch form

$$\Psi_{\mathbf{k}}(\mathbf{r}) = u_{\mathbf{k}}(\mathbf{r})e^{i\mathbf{k}\cdot\mathbf{r}} \quad (3.30)$$

where \mathbf{k} is the wavevector and $u_{\mathbf{k}}(\mathbf{r})$ is a function with the same periodicity of the lattice, that is $u_{\mathbf{k}}(\mathbf{r}) = u_{\mathbf{k}}(\mathbf{r} + \mathbf{R}_n)$. We can use this fact to expand $u_{\mathbf{k}}(\mathbf{r})$ in a Fourier series

$$u_{\mathbf{k}}(\mathbf{r}) = \sum_{\mathbf{G}} c_{\mathbf{k}+\mathbf{G}} e^{i\mathbf{G}\cdot\mathbf{r}} \quad (3.31)$$

where \mathbf{G} are reciprocal lattice vectors and $c_{\mathbf{k}+\mathbf{G}}$ are constants. The general solution of the Schrödinger equation is then

$$\Psi_{\mathbf{k}}(\mathbf{r}) = \sum_{\mathbf{G}} c_{\mathbf{k}+\mathbf{G}} e^{i(\mathbf{k}+\mathbf{G})\cdot\mathbf{r}} \quad (3.32)$$

Wavefunctions in the Bloch form are not only easier to manage, but they offer significant computational advantages. In fact, solving Eq. (3.21) requires solving many integrals of the form $\langle \Psi_{\mathbf{k}}(\mathbf{r}) | \hat{H} | \Psi_{\mathbf{k}}(\mathbf{r}) \rangle$, and for a given value of \mathbf{k} the integrals should be taken over the whole real space. Fortunately, if $\Psi_{\mathbf{k}}(\mathbf{r})$ is a Bloch function, it can be proven that the solution of the integral are given by the sum of the band energies ϵ_n , so

$$\langle \Psi_{\mathbf{k}}(\mathbf{r}) | \hat{H} | \Psi_{\mathbf{k}}(\mathbf{r}) \rangle = \frac{\Omega}{(2\pi)^3} \sum_n \int_{BZ} \epsilon_n(\mathbf{k}) d\mathbf{k} \quad (3.33)$$

where Ω is the volume of the unit cell and the integral is taken over the fist Brillouin zone. This integral is much easier to compute. In practical calculations, the integral over the Brillouin zone is evaluated only on a finite set of points. The most common

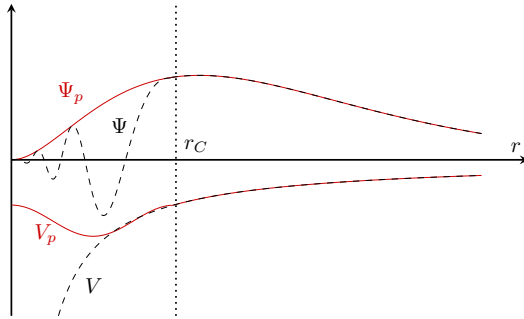


Figura 3.1: Comparison of a wavefunction in the Coulomb potential of the nucleus (black line) and in a pseudopotential (red line). The wavefunctions and potentials coincide for distances greater than r_C .

choice for this set of points is the Monkhorst-Pack grid [32]. In fractional coordinates, it is a rectangular grid spaced evenly throughout the Brillouin zone. The main advantage of this method is that it gives accurate results even with few points.

Sometimes, the integration has problems to converge because of the discontinuity points of the function. This is particularly common in metals, where it is common to have regions in the reciprocal space where the electronic density suddenly drops to zero. To avoid this inconvenience, the discontinuity regions are softened applying *smearing* functions. For example, it is common to use Gaussian functions centred in the discontinuity and parametrized by their standard deviation σ . In the limit $\sigma \rightarrow 0$ there is no smearing, and the discontinuity is not eliminated.

The problem of solving the Kohn-Sham equations is not completely solved yet. In fact, in Eq. (3.32) the sum is extended over an infinite number of reciprocal lattice vectors \mathbf{G} , so it is not possible to evaluate it exactly. Luckily, the single terms in the sum may be interpreted as solutions to the free-particle Schrödinger equation. To each term, we can associate an energy of

$$E_{\mathbf{k}} = \frac{\hbar^2(\mathbf{k} + \mathbf{G})^2}{2m} \quad (3.34)$$

The higher energy terms will have less physical meaning, so they can be excluded from the sum. This is done by choosing a cut-off value E_{cut} and a corresponding

$$G_{\text{cut}} = \sqrt{\frac{2mE_{\text{cut}}}{\hbar^2}} \quad (3.35)$$

The terms in the sum in Eq. (3.32) with $|\mathbf{G}| < G_{\text{cut}}$ are ignored.

Usually, in DFT applications, another simplification is made. Since most of the properties of materials are determined only by the valence electrons, the ion-electron interaction is determined using pseudopotentials. With pseudopotentials, the core

electrons are removed from the calculation, and they are replaced with an effective potential. Only the valence electrons (or the valence and outer core electrons) are simulated. In addition to reducing the number of electrons that have to be simulated, pseudopotentials offer a second advantage. The valence electrons wavefunctions oscillate rapidly near the nucleus because of the strong nuclear potential, as it can be seen in Fig. 3.1. The rapid oscillations in the region close to the nucleus require high frequency cut-off energies, impacting on the simulation performance. Pseudopotentials "smoothen" the wavefunctions, allowing to choose a smaller G_{cut} and making the computation faster.

3.3 VIENNA AB-INITIO SIMULATION PACKAGE

VASP is a computer program developed by the University of Vienna for DFT calculations [33–36]. This software has been used for all the simulations performed in this thesis. In this section, we will describe how a general simulation in VASP is performed.

Before performing a calculation, the basic elements that VASP needs are: the position of the atoms in the crystal, the k-space mesh grid to be used, and the pseudopotentials. Each of this element is given in input to the program through a different file. The first file is named POSCAR, and it contains a description of the crystal. An example is given below

```

1 Cubic diamond          # first line used as comment
2   5.5                  # lattice constant (in angstrom)
3 #--- Definition of the basis vectors of the primitive cell---
4   0.0   0.5   0.5      # a1
5   0.5   0.0   0.5      # a2
6   0.5   0.5   0.0      # a3
7 Si                      # atomic species
8 2                      # number of atoms in the primitive cell
9 #--- Positions of the atoms in the primitive cell---
10 Direct                 # Direct: lattice vectors basis
11                         # Cartesian: cartesian basis
12   0.00  0.00  0.00    # first atom
13   0.25  0.25  0.25    # second atom
14                         # [...]

```

The first half of the file describes the lattice. The lattice is defined through the three basis vectors \mathbf{a}_1 , \mathbf{a}_2 and \mathbf{a}_3 . These vectors are given by multiplying the lattice constants defined in line 2 with the vectors defined in lines 4-6. The second half of the file describes the composition of the primitive cell. Lines 7 and 8 define the type and number of atoms in the cell, whereas line 12-13 their positions. The positions can be expressed in cartesian coordinates (Cartesian) or in the lattice basis \mathbf{a}_1 , \mathbf{a}_2 , \mathbf{a}_3 (Direct).

The second file is named KPOINTS, and it describes the k-space grid. The grid can be automatically generated by VASP or given explicitly by the user. An example of the first case is given below

```

1 Automatic mesh      # first line used as comment
2 0                  # 0 stands for automatically generated
3 Monkhorst Pack   # generation method
4 11 11 11          # number of k-points in each direction
5 0 0 0             # optional shift of the mesh

```

The zero in line 2 indicates that the grid has to be generated automatically with the generation method specified in line 3. Line 4 gives the number of points that have to be generated in every direction and line 5 an optional shift with respect to the centre of the Brillouin zone. In our example, a Γ -centered $11 \times 11 \times 11$ grid is generated.

In band structure calculations, it is convenient to specify a custom grid. Instead of calculating the energy of the electrons for evenly-spaced k-points, some specific k-points of interest are chosen. Typically, they are special points of symmetry, like the centre of the Brillouin zone or the center of a side of the Fermi surface. An example is given below.

```

1 Bandstructure G-X-W-G          # first line used as comment
2 10                             # number of k-points per line
3 Line                           # line between the specified points
4 Reciprocal                      # Reciprocal or Cartesian
5 0.0 0.0 0.0    Gamma           # first point
6 0.5 0.5 0.0    X              # second point
7
8 0.5 0.5 0.0    X              # [...]
9 0.5 0.75 0.25   W
10
11 0.5 0.75 0.25   W
12 0.0 0.0 0.0    Gamma

```

In this example, three lines of 10 k-points are generated. The first goes from the point Γ to X, the second from X to W and the third from W to Γ . The number of points per line is defined in line 2. Like in the POSCAR, the points coordinates may be expressed in cartesian coordinates (Cartesian) or with respect to the reciprocal base $\mathbf{b}_1, \mathbf{b}_2, \mathbf{b}_3$ (Reciprocal).

The last file that defines the system is named POTCAR. It contains all the information about the pseudopotentials that have to be used for the atoms in the cell. If more than one type of atom is present, multiple POTCARs are concatenated in a unique file.

All the computational instructions, like the energy cut-off, are specified in the INCAR file. The INCAR file can contain a very vast number of parameters, of which giving a comprehensive description here would be impossible. We will present some of them in the next chapter, when we need to use them. A complete list of the tags that can be used in the INCAR file can be found in the VASP wiki [37].

SIMULATION OF A SMALL POLARON IN RUTILE

Rutile is the most common natural form of titanium dioxide (TiO_2). It is a material that has been vastly studied in the past decades [24]. It is known to be prone to the formation of small electron polarons, which give rise to an optically detected deep level below the conduction band. However, experiments seem to produce conflicting results: optical and spin-resonance techniques reveal strongly localized small polarons, while electrical measurements show high mobilities that can only be explained by delocalized free electrons. It was shown that small polarons can actually coexist with delocalized electrons in the conduction band of TiO_2 , the former being only slightly more energetically favoured over the latter [38].

In this chapter, we discuss the simulation of a small polaron in rutile. The DFT+U calculation was run on VASP on a $3 \times 3 \times 3$ supercell. We start by discussing the procedure that was followed to trap an extra electron in the TiO_2 supercell. Then, the resulting density of states and band structure are discussed. Particular emphasis is given to the comparison with a delocalized solution, where the electron enters the conduction band.

4.1 PROCEDURE

4.1.1 DFT and DFT+U calculation on rutile

We began by performing a standard DFT calculation on rutile. To do so, we first needed some information on the material we were investigating. Rutile has a tetragonal unit cell, with two titanium and four oxygen atoms inside. A sketch of the unit cell is shown in Fig. 4.1a. The lattice parameters and the positions of the atoms were taken from The Materials Project website [40] and inserted in the POSCAR file. The properties of the atoms, as discussed in Section 3.2, are described by pseudopotentials. For titanium atoms, a projector augmented wave (PAW) pseudopotential with 12 valence electrons ($3s^2 3p^6 4s^1 3d^3$) was used, whereas for oxygen atoms a PAW pseudopotential with 6 valence electrons ($2s^2 2p^4$) was chosen. For the k-points grid, we used a $7 \times 7 \times 11$ Γ -centered grid, with a spacing of about 0.03 \AA^{-1} .

With these settings, a series of DFT calculations was performed. In all the calculations we set the cut-off energy to 700 eV. The convergence process was stopped when both the energy difference between two successive electronic calculations was smaller than 10^{-8} eV and the forces acting on the ions were smaller than 0.01 eV/ \AA . A Gaussian smearing of $\sigma = 0.05$ was used for the calculations that involved the relaxation of

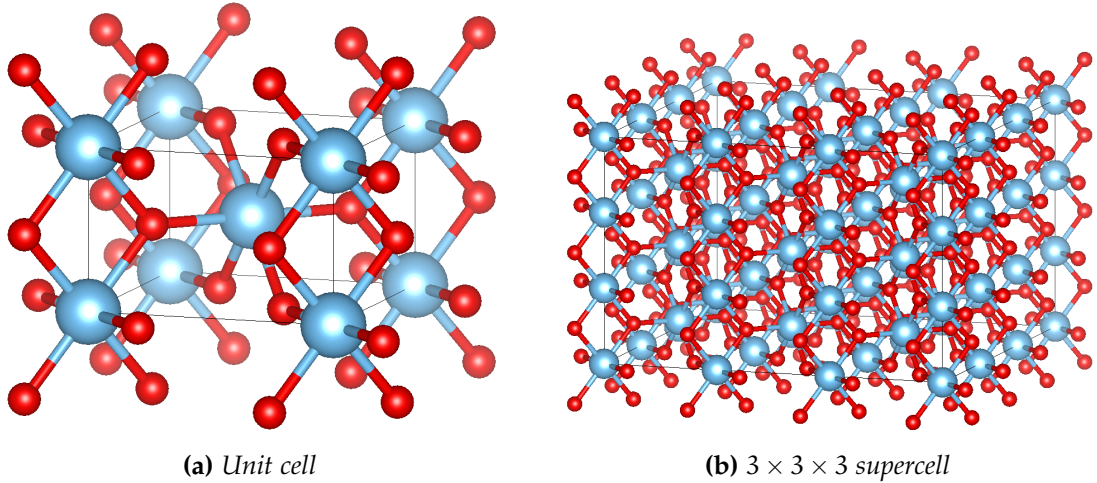


Figura 4.1: Rutile unit cell and supercell. Titanium is blue and oxygen is red. The images have been rendered with Vesta [39].

the lattice or the computation of the band structure. On the other hand, for the computation of the density of states (DOS), the tetrahedron smearing method was used. The tetrahedron method usually gives better results, but VASP does not implement it for calculations where the position of the ions changes.

Before investigating the electronic properties of the material, we wanted to be sure that the structure was properly relaxed. A non-spin-polarized calculation was performed on the unit cell in order to allow the relaxation of the ions positions. The volume and the shape of the unit cell was kept constant, allowing the atomic positions to change. This was achieved by performing a series of standard electronic DFT calculations. When electronic convergence is reached, the forces acting on the ions are computed, and the ions positions are updated minimizing the forces. Then, another electronic calculation is run. The process is stopped when both the electronic and the ionic calculations converge.

The relaxed structure was employed in a standard self-consistent DFT calculation. In particular, the DOS, the electronic charge density and the wavefunctions were computed. The result was used in a non-selfconsistent calculation to compute the band structure. The bands were calculated along a special path of k-points. Conventionally, these points are named Γ -X-M- Γ -Z-R-A-Z; X-R; M-A, and they are high-symmetry points of the first Brillouin zone of a tetragonal system. The positions of these points in the Brillouin zone are shown in Fig. 4.2. The path was created connecting each couple of high-symmetry k-points with a line of 10 evenly-spaced points.

As discussed in Section 3.1.3, DFT often fails to give appropriate results in band-gap calculations. To avoid the problem, the previous calculations were repeated in DFT+U. The DFT+U correction was implemented following the Duradev approach, setting the value of $U - J$ to 3.9 eV. This value was determined by Reticcioli et al. entirely from first

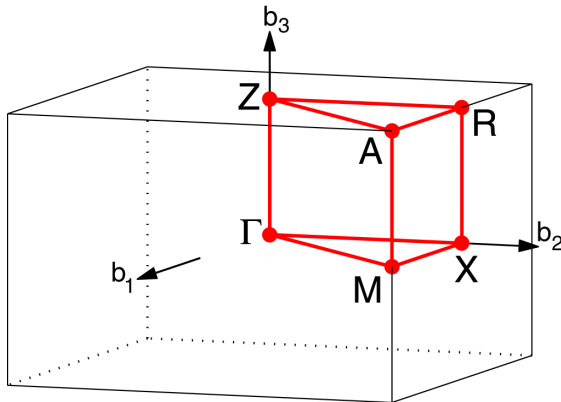


Figura 4.2: Brillouin zone of a tetragonal system, the red path passes through the high-symmetry points of the zone. $\mathbf{b}_1, \mathbf{b}_2, \mathbf{b}_3$ are the reciprocal basis vectors of a tetragonal unit cell. The path used in the calculation of the band structure was Γ -X-M- Γ -Z-R-A-Z; X-R; M-A.

principles [41], using the constrained random phase approximation (cRPA) [31]. The correction was applied to the titanium d-orbitals, leaving the other orbitals unaltered. In fact, as discussed in Section 3.1.3, s- and p-orbitals are less localized than d-orbitals, and they do not need corrections. Starting with the relaxed structure, we relaxed it again with the DFT+U correction. The DOS and band structure were computed as well, following the same procedure that was described above.

4.1.2 Electron localization

To find a polaronic solution, we had to add an extra electron to the system and localize it at the centre of the cell. Since the electron had to be localized in a region comparable with the size of a unit cell, the simulation could not be run on a unit cell alone. VASP, as many other DFT software packages, uses periodic boundary conditions, so the electron would interfere with itself at the cell boundaries. A large-enough supercell is needed to avoid self-interaction errors. For this reason, large polarons are hard to simulate in DFT: the supercell size makes the calculation computationally very expensive.

A $3 \times 3 \times 3$ supercell was created repeating the relaxed unit cell three times in each direction. The unit cell that was repeated was the result of the relaxation performed with the DFT+U correction. A sketch of the supercell is shown in Fig. 4.1b. Given the bigger size of the cell, to have k-points separated by 0.03 \AA^{-1} , a $2 \times 2 \times 4$ grid was enough. The usual calculations described above were performed on the supercell, computing the DOS and the band structure.

Since the formation of the polaron is only slightly energetically favoured compared to a delocalized solution, the extra electron was difficult to localize. Adding one electron to the system does not result in a localized state, but in an electron delocalized in the

whole supercell. To find a localized solution, a more gradual approach was necessary.

The central titanium atom was substituted with vanadium, which is the element following titanium in the periodic table. Given its higher atomic number, it has one more electron and a stronger nuclear attraction. The position of the new atom was set in the POSCAR file, and a vanadium PAW pseudopotential with 13 valence electrons ($3s^23p^64s^13d^4$) was added to the POTCAR file. Added the electron, a number of expedients was needed to ensure its localization. The aim was to localize it on the central atom, the vanadium one. The six oxygen atoms around the central atom were moved outwards by 0.04 Å, creating a potential well for the electron. The distortion of the lattice broke the symmetry of the system, and since VASP usually takes advantage of the symmetry of the system to fasten calculations, this feature was disabled. The $U - J$ value was set to 3.9 eV for the titanium d-orbitals and to 9 eV for the vanadium d-orbitals. Together, the stronger nuclear attraction, the displacement of the oxygen atoms, and the high $U - J$ value, favoured the electron localization on the central atom.

A DFT+U calculation with lattice relaxation was run. Since the extra electron introduced a spin magnetic moment to the system, the calculation was spin-polarized. The magnetic moment was initially set to zero for every atom except for the vanadium one, for which it was set to $+\mu_B$, where μ_B is the Bohr magneton. To check if the electron localization was successful, the magnetic moments of the atoms were inspected. For a localized state, we expected the central vanadium atom to be the only one with a magnetic moment of the order of μ_B . On the other hand, for a delocalized state, we expected the extra magnetic moment introduced by the additional electron to be spread on all the atoms of the supercell.

The localized solution was used to initialize a new set of calculations. The goal was to gradually substitute the vanadium atom with a high $U - J$ value with a titanium atom with a normal $U - J$ value. This was done in two steps.

Firstly, vanadium was removed and titanium was placed back, leaving the $U - J$ value applied to the central atom to 9 eV. The number of electrons was manually set to the same number of the calculation with vanadium. The atomic positions were initialized as in the previous calculations, with the oxygen atoms shifted by 0.04 Å. The calculation was started with the charge density and wavefunctions obtained with vanadium, where the additional electron was already localized. The calculation was spin-polarized, and the initial magnetic moment was read from the charge density file. The localization of the extra electron was checked looking at the magnetic moment of the atoms as explained above. The eigenvalues and DOS were also inspected to see if a new state was present in the middle of the band gap.

Secondly, the calculation of the polaron was done continuing the last calculation with a $U - J$ value of 3.9 eV. The calculation was initialized with the atomic positions, charge density and wavefunctions of the previous calculation. The magnetic moments, DOS and eigenvalues were inspected again to check if the polaron was present.

4.1.3 Polaron

Different calculations were run to compute some of the polaron properties. A static electronic calculation was run starting from the previous result to compute a more precise DOS. The band structure of the polaronic solution was also computed with a non-self-consistent calculation on the usual path of k-points. Finally, the isosurfaces of the polaron charge density were computed. To do so, the charge density was decomposed over the different bands, and the contribution of the polaron was selected restricting the energy to an appropriate interval. The final result was rendered with Vesta, and the electron localization observed.

A delocalized solution was computed as well for comparison. To achieve this, an extra electron was added to the supercell and a non-spin-polarized DFT+U calculation was performed. The extra electron was added manually, setting the number of electrons to the number of the electrons in the original rutile supercell plus one. The DOS and band structure were computed and compared with the polaronic solution.

4.2 RESULTS AND DISCUSSION

4.2.1 DFT and DFT+U calculation on rutile

The results of the DFT and DFT+U calculations on the rutile unit cell are reported in Fig. 4.3. In the diagrams, the zero of the energy has been shifted to the top of the highest valence band, so that all the electrons are situated in the region $E < 0$. An energy gap is clearly visible both in the band structure and in the DOS. The band gap is found to be direct, meaning that both the top of the highest valence band and the bottom of the lowest conduction band are found in correspondence of the same k-point; here it is the Γ k-point. As expected, the energy gap is larger in the DFT+U calculation. The standard DFT calculation returned a gap of 1.83 eV, whereas the DFT+U calculation a gap of 2.33 eV.

In Fig. 4.4, the band structure and the DOS of the rutile supercell are reported. We expected the band structure and the DOS of the supercell to be very similar to the unit cell ones, the main difference being that in the supercell many more bands are accessible. This is due to the bigger number of atoms, since each individual atom contributes to the total band structure with its own atomic orbitals. Band-unfolding techniques have been developed to overcome this inconvenience, reducing the supercell band structure to the unit cell one [42]. However, since the exact band structure of rutile was not the main focus of this work, these techniques were not employed. Nevertheless, in Fig. 4.4 we can still clearly see a band structure and a DOS similar to the ones observed in Fig. 4.3b. The energy gap is of 2.33 eV, as it was for the unit cell in the DFT+U calculation. In both diagrams, the DOS has been divided by the total number of atoms N to make the results comparable.

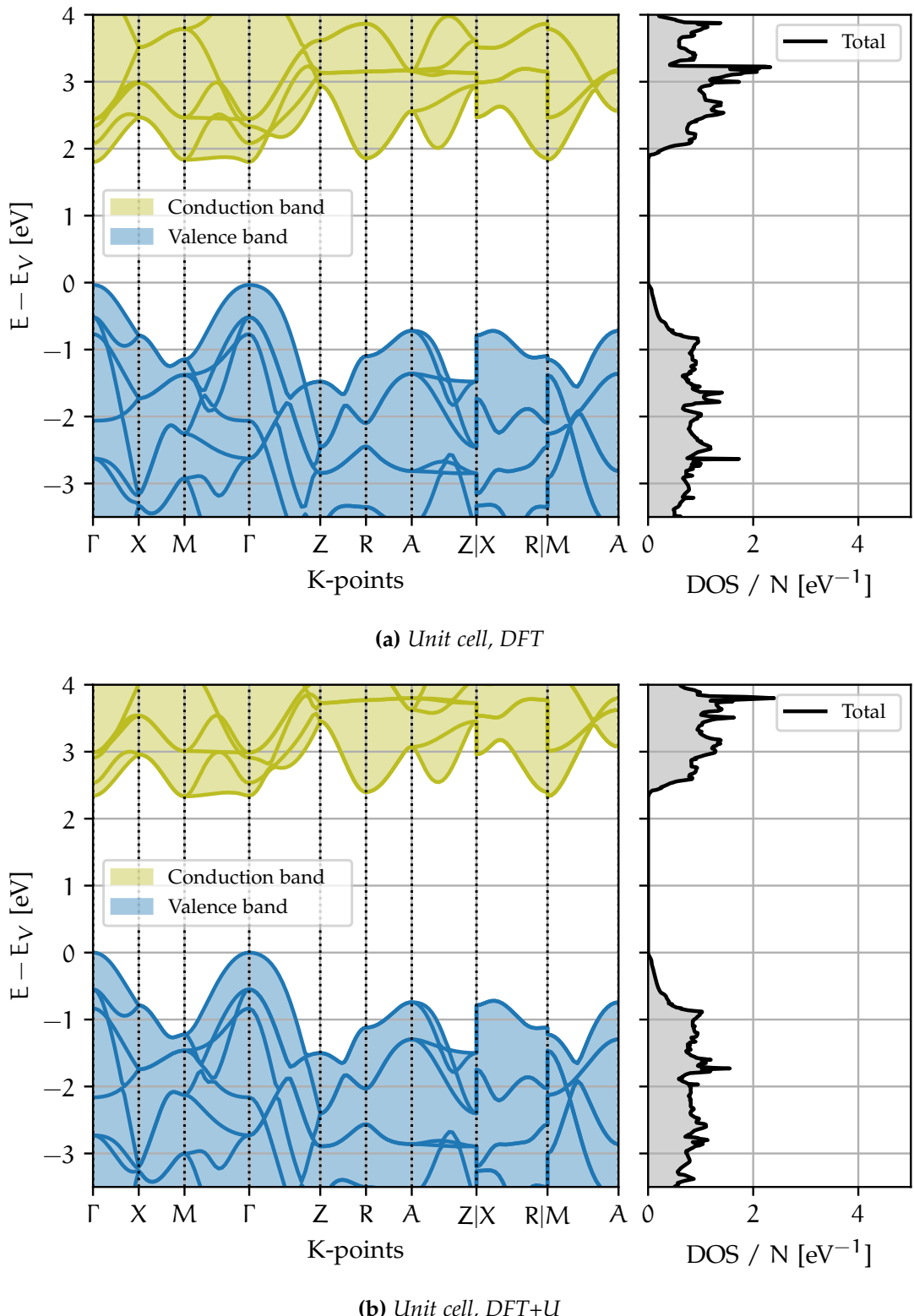


Figura 4.3: Band structure and DOS of the rutile unit cell. The zero of the energy has been shifted to the top of the highest valence band E_V . The DOS is divided by the total number of atoms $N = 6$. The direct $\Gamma - \Gamma$ energy gap in (a) is of 1.83 eV, whereas in (b) it is of 2.33 eV.

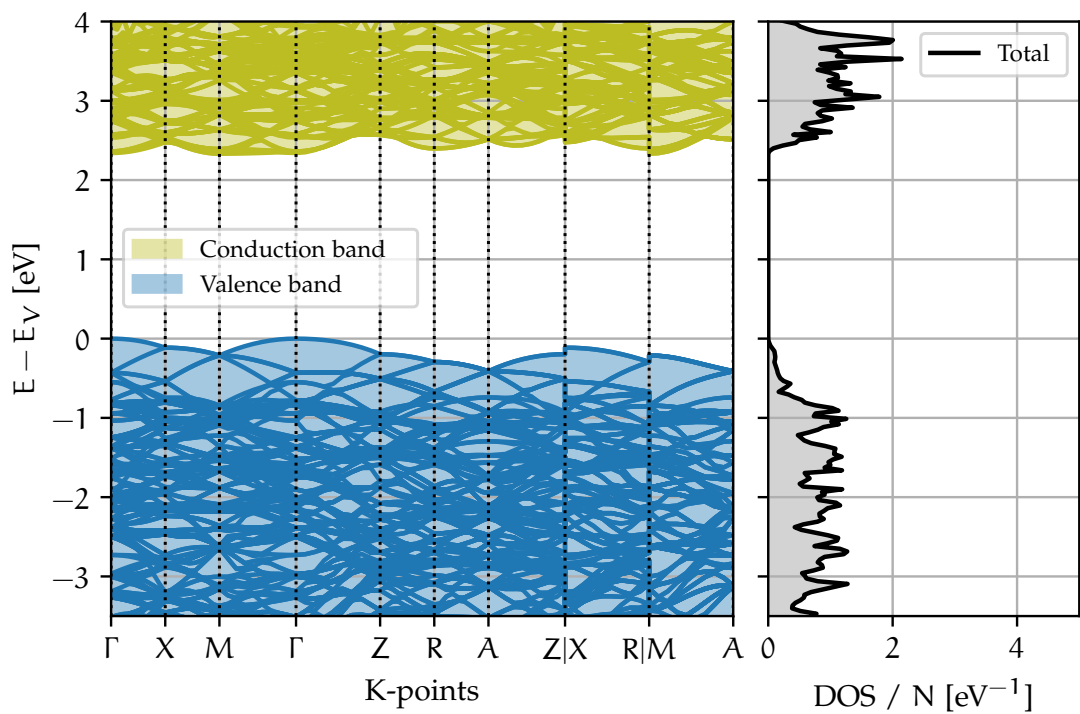


Figura 4.4: Band structure and DOS of the rutile supercell. The zero of the energy has been shifted to the top of the highest valence band E_V . The DOS is divided by the total number of atoms $N = 162$. The direct $\Gamma - \Gamma$ energy gap is of 2.33 eV.

4.2.2 Electron localization

The localization of the extra electron was successful: the electron localized on the vanadium atom and remained localized at the centre of the supercell in the following steps. The localization on the central vanadium atom was clearly visible from the eigenvalues, since a new state with spin +1/2 was found in the conduction band. The vanadium atom was the only one with a magnetic moment different from zero, equal to $1.093\mu_B$. After the substitution of vanadium with titanium, with a $U - J$ value of 9 eV, the localization was confirmed by a magnetic moment on the central atom of $0.930\mu_B$. Finally, setting $U - J$ to 3.9 eV, the electron remained localized. The magnetic moment on the central titanium atom was $0.787\mu_B$.

4.2.3 Polaron

The DOS and the band structure of the polaronic solution are reported in Fig. 4.5a. An extra state is clearly visible both in the DOS and in the band structure, 0.70 eV below the conduction band. This is compatible with the expectations for small polarons, which usually create a new state approximately 1 eV below the conduction band. In the DOS diagram, the total DOS has been plotted together with its projection on the central titanium atom. It is interesting to pay attention to the region between -0.2 eV and 0.0 eV, where the polaronic state can be found. Here, most of the contribution to the total DOS is given by the projection on the central atom, meaning that the electron is mostly localized on this atom.

The previous plot can be compared with Fig. 4.5b, where the delocalized solution is shown. We notice that the zero of the energy is shifted up to the bottom of the conduction band, which now coincides with the top of the valence band. Both the band structure and the DOS show that the extra electron enters the conduction band, and that no new state is created in the middle of the energy gap. The contribution of the central atom to the total DOS is not as relevant as before. This is compatible with an electron delocalized in the material, where the central atom does not play any particular role.

The two cases can also be compared looking at the charge isosurfaces. The total charge density was projected on the band of the extra electron. The result is displayed in Fig. 4.6 for the entire supercell and in Fig. 4.7 with a focus on the central atom. From Fig. 4.6a it is clearly visible how in the polaronic case the charge is localized at the centre of the supercell. The exact shape of the charge isosurface is better visible in Fig. 4.7a. Here it is also emphasized how the localization of the charge is possible only thanks to the displacement of the oxygen atoms. The four oxygen atoms closer to the titanium atom are displaced by 0.085 Å outwards, whereas the two further oxygen atoms by 0.023 Å. In the delocalized case, displayed in Figs. 4.6b and 4.7b, the electron is delocalized both on the titanium and oxygen atoms.

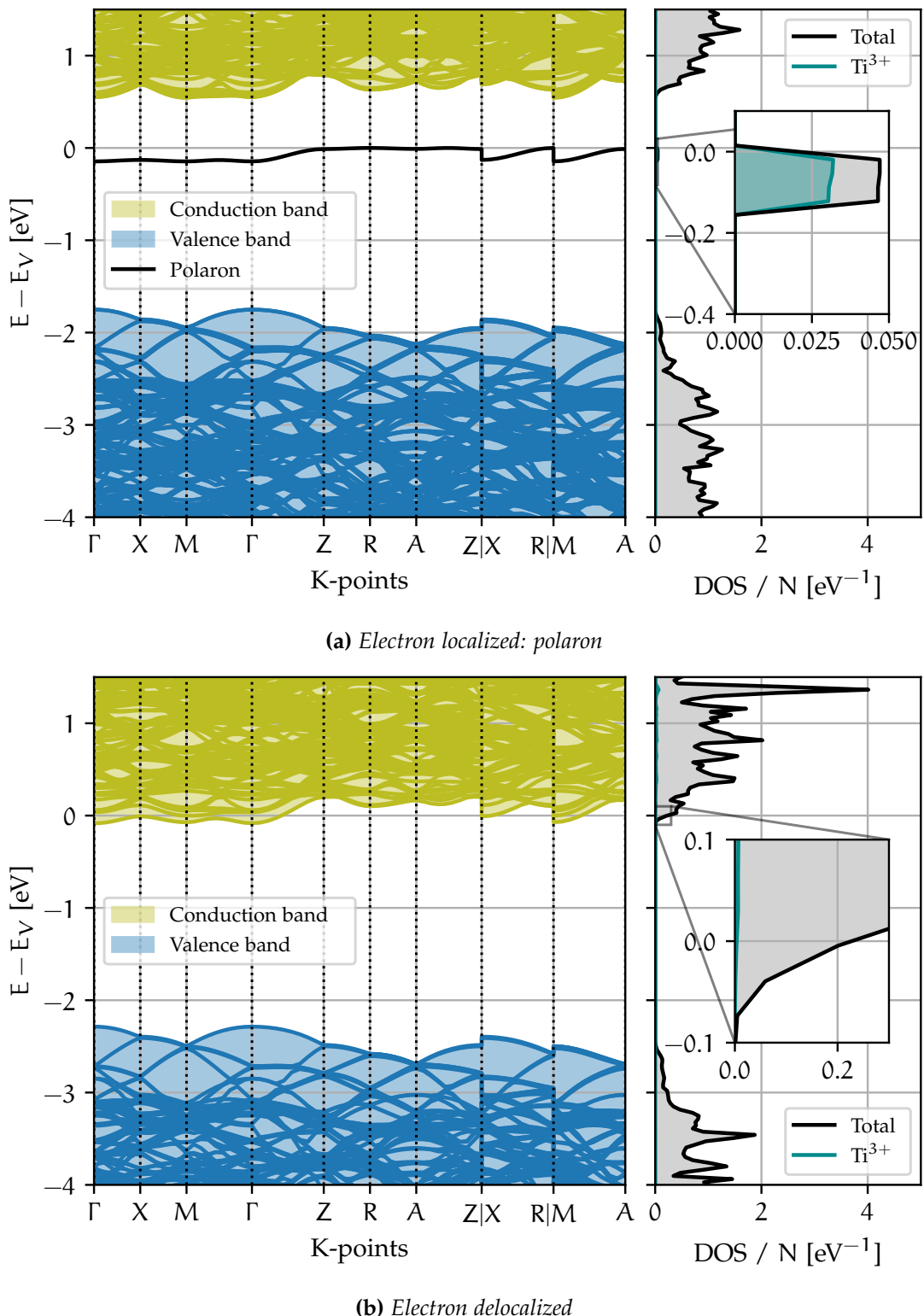


Figura 4.5: Band structure and DOS of the rutile supercell with an extra electron. The zero of the energy has been shifted to the top of the highest valence band E_V . The DOS is divided by the total number of atoms $N = 162$. In addition to the total DOS, the partial DOS of the central atom is reported as well.

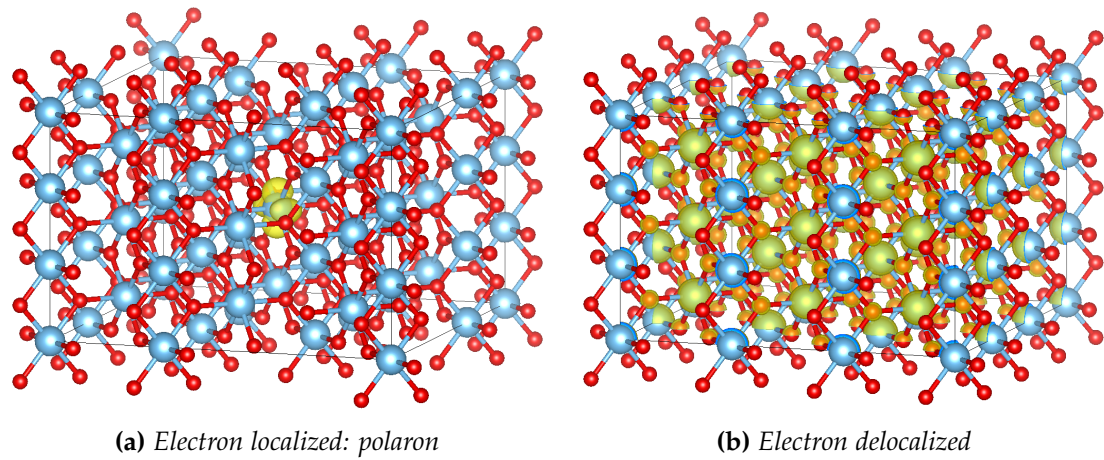


Figura 4.6: Supercell with the isosurface (10%) of the charge density projected on the extra-electron band. In (a) the extra electron is localized and forms a polaron, in (b) it is delocalized. The blue atoms are titanium atoms, whereas the red ones are oxygen atoms.

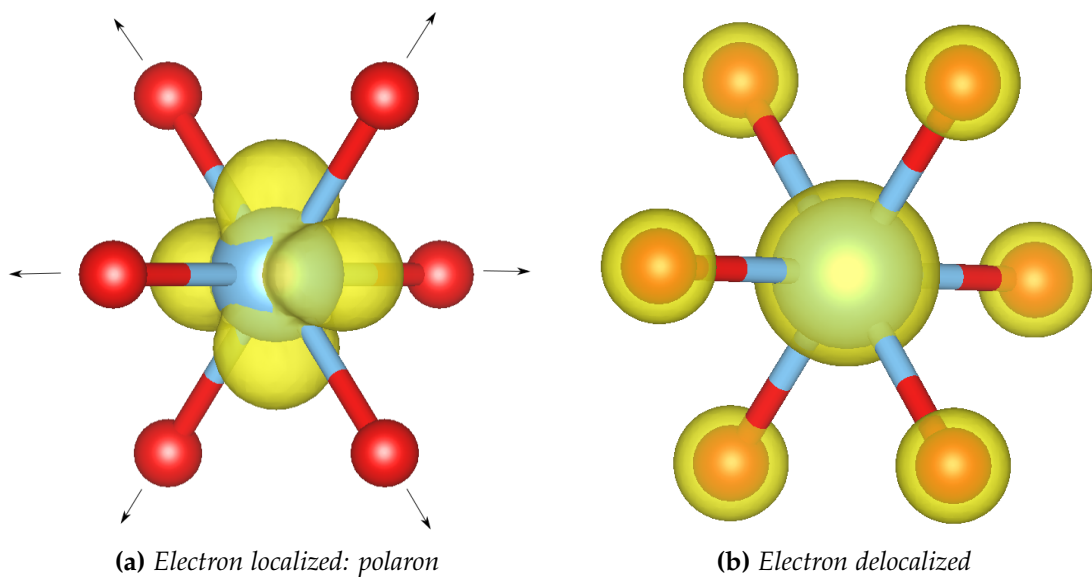


Figura 4.7: Central atom with the isosurface (10%) of the charge density projected on the extra-electron band. In (a) the extra electron is localized and forms a polaron, in (b) it is delocalized. The blue atom is the central titanium atom, whereas the red ones are the nearest-neighbours oxygen atoms.

CONCLUSIONS

We started by introducing polarons at a general level, following the main historical steps that brought to the present understanding of these quasi-particles. Landau was the first to propose the concept of an electron localized in a self-generated potential well. In collaboration with Pekar, they proposed a first model to describe this new quasi-particle. Fröhlich and Holstein expanded their work proposing a description of polarons based on a quantum treatment of the lattice polarization. Fröhlich and Holstein Hamiltonians are currently used for the characterization of large and small polarons, respectively. These two types of polarons are characterized by the size of the polarization region, respectively larger and smaller than the unit cell. They also differ in their properties. In particular, we focused on the depth of their energy level and their mobility. The new energy level is formed $\simeq 10$ meV below the conduction band for large polarons and $\simeq 1$ eV below the conduction band for small polaron. The mobility is larger and decreasing with temperature for large polarons and smaller and increasing with temperature for small polarons.

In the second part of the thesis, we focused on numerical techniques useful for the simulation of small polarons. We presented the DFT formalism, describing its advantages and its flaws. A correction of it, DFT+U, was presented as well, together with its implementation in the Vienna Ab Initio Simulation Package. VASP was used for the simulation of a small polaron trapped in rutile. The calculation was described in detail, focusing on the method used to localize the electron at the centre of the supercell. The results were then briefly discussed. A new energy level was found 0.70 eV below the conduction band, and the charge of the extra electron was found to be localized on the atom at the centre of the supercell. This solution was compared with the solution found for an extra electron delocalized in the cell. The delocalized electron enters the conduction band and its charge is delocalized on the whole cell.

The results were compatible with the expectations, at least at a qualitative level. The simulation could be improved proposing a quantitative comparison with the literature. The band structure of the supercell could be reduced to the unit cell one applying band-unfolding techniques. The effective mass and the formation energy of the polaron could be computed as well. With compatible results, the work could be extended to the simulation of a small polaron in a new material, trying to determine if it is prone to the formation of polarons or not.

BIBLIOGRAFIA

- [1] "Electron Motiton in Crystal Lattice". In: *Collected Papers of L.D. Landau*. A cura di D. Ter haar. Pergamon, 1 gen. 1965, pp. 67–68. ISBN: 978-0-08-010586-4. DOI: [10.1016/B978-0-08-010586-4.5.00015-8](https://doi.org/10.1016/B978-0-08-010586-4.5.00015-8) (cit. a p. vii).
- [2] Solomon Pekar. "Local Quantum States of Electrons in an Ideal Ion Crystal". In: *Zhurnal Eksperimentalnoi i Teoreticheskoi Fiziki* 16.4 (1946), pp. 341–348 (cit. a p. vii).
- [3] S. I. Pekar. "Theory of Colored Crystals". In: *Zhurnal Eksperimentalnoi i Teoreticheskoi Fiziki* 17 (1947), p. 868 (cit. a p. vii).
- [4] L. D. Landau e S. I. Pekar. "Effective Mass of a Polaron". In: *Zh. Eksp. Teor. Fiz.* 18.5 (1948), pp. 419–423 (cit. alle pp. vii, 20).
- [5] Herbert Fröhlich, Hans Pelzer e Sigurd Zienau. "XX. Properties of Slow Electrons in Polar Materials". In: *The London, Edinburgh, and Dublin Philosophical Magazine and Journal of Science* 41.314 (1950), pp. 221–242 (cit. alle pp. vii, 20).
- [6] Th Holstein. "Studies of Polaron Motion: Part I. The Molecular-Crystal Model". In: *Annals of physics* 8.3 (1959), pp. 325–342 (cit. alle pp. vii, 30).
- [7] Han Rongsheng, Lin Zijing e Wang Kelin. "Exact Solutions for the Two-Site Holstein Model". In: *Physical Review B* 65.17 (16 apr. 2002), p. 174303. DOI: [10.1103/PhysRevB.65.174303](https://doi.org/10.1103/PhysRevB.65.174303) (cit. a p. vii).
- [8] Nikolai V. Prokof'ev e Boris V. Svistunov. "Polaron Problem by Diagrammatic Quantum Monte Carlo". In: *Physical Review Letters* 81.12 (21 set. 1998), pp. 2514–2517. DOI: [10.1103/PhysRevLett.81.2514](https://doi.org/10.1103/PhysRevLett.81.2514) (cit. a p. vii).
- [9] A. S. Mishchenko et al. "Diagrammatic Quantum Monte Carlo Study of the Fr\"ohlich Polaron". In: *Physical Review B* 62.10 (1 set. 2000), pp. 6317–6336. DOI: [10.1103/PhysRevB.62.6317](https://doi.org/10.1103/PhysRevB.62.6317) (cit. a p. vii).
- [10] Sebastian Kokott et al. "First-Principles Supercell Calculations of Small Polarons with Proper Account for Long-Range Polarization Effects". In: *New Journal of Physics* 20.3 (mar. 2018), p. 033023. ISSN: 1367-2630. DOI: [10.1088/1367-2630/aaaf44](https://doi.org/10.1088/1367-2630/aaaf44) (cit. a p. vii).
- [11] Weng Hong Sio et al. "Polarons from First Principles, without Supercells". In: *Physical Review Letters* 122.24 (19 giu. 2019), p. 246403. DOI: [10.1103/PhysRevLett.122.246403](https://doi.org/10.1103/PhysRevLett.122.246403) (cit. alle pp. vii, 34).
- [12] P. A. M. Dirac. "The Quantum Theory of the Emission and Absorption of Radiation". In: *Proceedings of the Royal Society of London Series A* 114 (1 mar. 1927), pp. 243–265. ISSN: 0080-46301364-5021. DOI: [10.1098/rspa.1927.0039](https://doi.org/10.1098/rspa.1927.0039) (cit. a p. 1).

- [13] V. Fock. "Konfigurationsraum und zweite Quantelung". In: *Zeitschrift für Physik* 75.9 (1 set. 1932), pp. 622–647. ISSN: 0044-3328. doi: [10.1007/BF01344458](https://doi.org/10.1007/BF01344458) (cit. a p. 1).
- [14] J. J. Sakurai e Jim Napolitano. *Modern Quantum Mechanics*. Cambridge University Press, 17 set. 2020. 571 pp. ISBN: 978-1-108-47322-4 (cit. a p. 6).
- [15] A. Sommerfeld. "Zur Elektronentheorie der Metalle auf Grund der Fermischen Statistik". In: *Zeitschrift für Physik* 47.1 (1 gen. 1928), pp. 1–32. ISSN: 0044-3328. doi: [10.1007/BF01391052](https://doi.org/10.1007/BF01391052) (cit. a p. 8).
- [16] P. Drude. "Zur Elektronentheorie Der Metalle; II. Teil. Galvanomagnetische Und Thermomagnetische Effecte". In: *Annalen der Physik* 308.11 (1900), pp. 369–402. ISSN: 1521-3889. doi: [10.1002/andp.19003081102](https://doi.org/10.1002/andp.19003081102) (cit. a p. 8).
- [17] Felix Bloch. "Über die Quantenmechanik der Elektronen in Kristallgittern". In: *Zeitschrift für Physik* 52.7 (1 lug. 1929), pp. 555–600. ISSN: 0044-3328. doi: [10.1007/BF01339455](https://doi.org/10.1007/BF01339455) (cit. a p. 9).
- [18] Marvin L. Cohen e Steven G. Louie. *Fundamentals of Condensed Matter Physics*. 1^a ed. Cambridge University Press. ISBN: 978-0-521-51331-9 (cit. a p. 14).
- [19] Jacques Tempere. *Advanced Electronic Structures*. Universiteit Antwerpen (cit. a p. 14).
- [20] Charles Kittel. *Quantum Theory of Solids*. Wiley, 2 apr. 1987. 528 pp. ISBN: 978-0-471-62412-7 (cit. alle pp. 16, 20).
- [21] A. S Alexandrov e J. T Devreese. *Advances in Polaron Physics*. Heidelberg; New York: Springer, 2010. ISBN: 978-3-642-01896-1 (cit. a p. 19).
- [22] Amin Tayebi e Vladimir Zelevinsky. "The Holstein Polaron Problem Revisited". In: *Journal of Physics A: Mathematical and Theoretical* 49.25 (mag. 2016), p. 255004. ISSN: 1751-8121. doi: [10.1088/1751-8113/49/25/255004](https://doi.org/10.1088/1751-8113/49/25/255004) (cit. a p. 31).
- [23] Yuriy Natanzon, Amram Azulay e Yaron Amouyal. "Evaluation of Polaron Transport in Solids from First-principles". In: *Israel Journal of Chemistry* 60.8-9 (2020), pp. 768–786. ISSN: 1869-5868. doi: [10.1002/ijch.201900101](https://doi.org/10.1002/ijch.201900101) (cit. a p. 33).
- [24] Cesare Franchini et al. "Polarons in Materials". In: *Nature Reviews Materials* 6.7 (1 lug. 2021), pp. 560–586. ISSN: 2058-8437. doi: [10.1038/s41578-021-00289-w](https://doi.org/10.1038/s41578-021-00289-w) (cit. alle pp. 33, 34, 45).
- [25] P. Hohenberg e W. Kohn. "Inhomogeneous Electron Gas". In: *Physical Review* 136 (3B 9 nov. 1964), B864–B871. doi: [10.1103/PhysRev.136.B864](https://doi.org/10.1103/PhysRev.136.B864) (cit. a p. 35).
- [26] W. Kohn e L. J. Sham. "Self-Consistent Equations Including Exchange and Correlation Effects". In: *Physical Review* 140 (4A 15 nov. 1965), A1133–A1138. doi: [10.1103/PhysRev.140.A1133](https://doi.org/10.1103/PhysRev.140.A1133) (cit. a p. 35).

- [27] A. Seidl et al. "Generalized Kohn-Sham Schemes and the Band-Gap Problem". In: *Physical Review B* 53.7 (15 feb. 1996), pp. 3764–3774. DOI: [10.1103/PhysRevB.53.3764](https://doi.org/10.1103/PhysRevB.53.3764) (cit. a p. 40).
- [28] Sarah Tolba et al. "The DFT+U: Approaches, Accuracy, and Applications". In: 16 mag. 2018. ISBN: 978-1-78923-132-8. DOI: [10.5772/intechopen.72020](https://doi.org/10.5772/intechopen.72020) (cit. a p. 40).
- [29] Vladimir I. Anisimov, Jan Zaanen e Ole K. Andersen. "Band Theory and Mott Insulators: Hubbard U Instead of Stoner I". In: *Physical Review B* 44.3 (15 lug. 1991), pp. 943–954. DOI: [10.1103/PhysRevB.44.943](https://doi.org/10.1103/PhysRevB.44.943) (cit. a p. 40).
- [30] S. L. Dudarev et al. "Electron-Energy-Loss Spectra and the Structural Stability of Nickel Oxide: An LSDA+U Study". In: *Physical Review B* 57.3 (15 gen. 1998), pp. 1505–1509. DOI: [10.1103/PhysRevB.57.1505](https://doi.org/10.1103/PhysRevB.57.1505) (cit. a p. 40).
- [31] F. Aryasetiawan et al. "Calculations of Hubbard \$U\$ from First-Principles". In: *Physical Review B* 74.12 (13 set. 2006), p. 125106. DOI: [10.1103/PhysRevB.74.125106](https://doi.org/10.1103/PhysRevB.74.125106) (cit. alle pp. 41, 47).
- [32] Hendrik J. Monkhorst e James D. Pack. "Special Points for Brillouin-zone Integrations". In: *Physical Review B* 13.12 (15 giu. 1976), pp. 5188–5192. DOI: [10.1103/PhysRevB.13.5188](https://doi.org/10.1103/PhysRevB.13.5188) (cit. a p. 42).
- [33] G. Kresse e J. Hafner. "Ab Initio Molecular Dynamics for Liquid Metals". In: *Physical Review B* 47.1 (1 gen. 1993), pp. 558–561. DOI: [10.1103/PhysRevB.47.558](https://doi.org/10.1103/PhysRevB.47.558) (cit. a p. 43).
- [34] G. Kresse e J. Furthmüller. "Efficiency of Ab-Initio Total Energy Calculations for Metals and Semiconductors Using a Plane-Wave Basis Set". In: *Computational Materials Science* 6.1 (1 lug. 1996), pp. 15–50. ISSN: 0927-0256. DOI: [10.1016/0927-0256\(96\)00008-0](https://doi.org/10.1016/0927-0256(96)00008-0) (cit. a p. 43).
- [35] G. Kresse e J. Furthmüller. "Efficient Iterative Schemes for Ab Initio Total-Energy Calculations Using a Plane-Wave Basis Set". In: *Physical Review B* 54.16 (15 ott. 1996), pp. 11169–11186. DOI: [10.1103/PhysRevB.54.11169](https://doi.org/10.1103/PhysRevB.54.11169) (cit. a p. 43).
- [36] G. Kresse e D. Joubert. "From Ultrasoft Pseudopotentials to the Projector Augmented-Wave Method". In: *Physical Review B* 59.3 (15 gen. 1999), pp. 1758–1775. DOI: [10.1103/PhysRevB.59.1758](https://doi.org/10.1103/PhysRevB.59.1758) (cit. a p. 43).
- [37] *The VASP Manual - Vaspwiki*. URL: https://www.vasp.at/wiki/index.php/The_VASP_Manual (visitato il 26/04/2022) (cit. a p. 44).
- [38] A. Janotti et al. "Dual Behavior of Excess Electrons in Rutile TiO₂". In: *physica status solidi (RRL) – Rapid Research Letters* 7.3 (2013), pp. 199–203. ISSN: 1862-6270. DOI: [10.1002/pssr.201206464](https://doi.org/10.1002/pssr.201206464) (cit. a p. 45).
- [39] *VESTA*. URL: <https://jp-minerals.org/vesta/en/> (visitato il 26/04/2022) (cit. a p. 46).

- [40] Kristin Persson. *Materials Data on TiO₂ (SG:136) by Materials Project*. United States, nov. 2014. DOI: [10.17188/1184648](https://doi.org/10.17188/1184648) (cit. a p. 45).
- [41] Michele Reticcioli, Ulrike Diebold e Cesare Franchini. “Modeling Polarons in Density Functional Theory: Lessons Learned from TiO₂”. In: *Journal of Physics: Condensed Matter* 34.20 (18 mag. 2022), p. 204006. ISSN: 0953-8984, 1361-648X. DOI: [10.1088/1361-648X/ac58d7](https://doi.org/10.1088/1361-648X/ac58d7) (cit. a p. 47).
- [42] Sara G. Mayo, Felix Yndurain e Jose M. Soler. “Band Unfolding Made Simple”. In: *Journal of Physics: Condensed Matter* 32.20 (feb. 2020), p. 205902. ISSN: 0953-8984. DOI: [10.1088/1361-648X/ab6e8e](https://doi.org/10.1088/1361-648X/ab6e8e) (cit. a p. 49).